To the Graduate Council:

I am submitting herewith a thesis written by Jofa Gideon Mwakisege entitled "The synthesis and stability of endohedral actinium-225($^{225}Ac@C_{60}$)". I have examined the final hard copy of this thesis for form and content and recommend that it be accepted in partial fulfillment of the requirements for the degree of Master of Science, with a major in Chemistry.

George Schweitzer, Major Professor

We have read this thesis
And recommend its acceptance:

George Kabalka

Jamie Adcock

Accepted for the Council:

Carolyn R. Hodges, Vice Provost
and Dean of the Graduate School

THE SYNTHESIS AND STABILITY OF ENDOHEDRAL ACTINIUM- 225 ($^{225}A_C@C_{60}$)

A Thesis
Presented for the
Master of Science
Degree

The University of Tennessee, Knoxville

Jofa Gideon Mwakisege

August 2008

DEDICATION

This thesis is dedicated to my parents

Mr. and Mrs. Mwakisege

Who has loved and inspired me throughout my life.

ACKNOWLEDGEMENTS

I would like to thank my research advisor, Dr. George Schweitzer for his input in the writing of this thesis. His involvement in my work has nourished my intellectual maturity such that I will be benefited for many years to come.

I offer my sincerest gratitude to my supervisor Dr. Mirzadeh, for the patience, knowledge and resources that he has extended in me. He has been my inspiration and has enriched my growth as a student, a researcher and scientist.

Many thanks to Dr. Musfeldt and Dr. Xue who have granted me time in the midst of their very busy schedules to accept and be part of this thesis.

I would also like to give my full appreciation to Dr. Rose Boll, Dr. Mike Dienner, Dr. Russ Knapp, John Cosgrove, Eric Dadush and Henry Lovett for the time and resources that they invested in me during my time in ORNL.

Beyond the chemistry world, I would like to thank my family members, my parents, my brothers; Joe, Jospa, Josia, Jogen and my sisters; Jogina, Josina and Joa for their support and encouragement.

I acknowledge the Department of Energy for their financial support during this project.

ABSTRACT

Due to their chemical and thermodynamic stability, fullerenes could play an important role in encapsulation of radionuclides for applications in radio-immunotherapy. In this thesis, we report the first synthesis of actinium endohedral fullerenes. The alpha-emitter Actinium-225 (^{225}Ac, $t_{1/2}$ =10 d) was trapped in fullerenes by the direct current (D.C) arc discharge-catcher method in a He atmosphere. Endohedral ^{225}Ac and the bulk of fullerene C_{60} was dissolved from the catcher electrode (a Pt disk covered with a thin layer of C_{60}) in toluene under N_2, and converted to the malonic ester derivative. Repeated washing of the organic phase with dilute HNO_3 demonstrated that a small fraction of ^{225}Ac (1.0 %) could not be removed from the organic phase and presumably was inside the fullerenes. The Fr- 221 (the α-decay daughter of ^{225}Ac), however, was observed to be leaking from the cage probably as a result of nuclear recoil. The cage stability was enhanced significantly by coupling the fullerene surface with organic adducts. After repetitive extractions, a 45% fraction of original activity was still retained in the cage. The radioactivity distribution coefficients {Kd = (^{225}Ac radioactivity in aqueous- phase)/ (^{225}Ac radioactivity in organic phase)} were investigated. We propose that, if Kd and back to back extractions, collectively are to be study in timely manner, the rate in which $^{225}Ac@C_{60}$ dissociate into individual components would be obtained.

TABLE OF CONTENTS

CHAPTER 1 INTRODUCTION 1
1.1 Why C60 (fullerene) 1
1.2 Why ^{225}Ac? 3
1.3 Broad Spectrum 3

CHAPTER 2 EXPERIMENTAL 7
2.1 Materials and chemicals 7
2.3 Radioactivity Measurements 9
2.4 Thin Layer Chromatography-Biocanner 13
2.5 High Performance Liquid Chromatography (HPLC) 14
2.6 Mass Spectrometry 15
2.7 Artists Air Brush 16
2.8 Electroplating 17
2.9 Recoil Catcher Apparatus / Arc Chamber 18

CHAPTER 3 EXPERIMENTAL PROCEDURE 20
3.1 Fullerene Catcher Disk 20
3.2 Process for Electroplating of ^{225}Ac 20
3.3 Procedure for the Insertion of ^{225}Ac into C_{60} via Electrical Arc 21
3.4 Procedure for the Extraction of ^{225}Ac from the Organic Phase 22
3.5 Procedure to Investigate the Fate of ^{221}Fr upon Decay of ^{225}Ac@C_{60} 22
3.6 Procedure for Fullerene Surface Modification 23
3.7 Removal of Exohedral ^{225}Ac 23

CHAPTER 4 RESULTS 25
4.1 Electroplating 25
4.2 Extractions 29
4.3 Chromatography 33

CHAPTER 5 DISCUSSION AND CONCLUSION 52
5.1 Discussion 52
5.2 Conclusion 58

REFERENCE 60

VITA 63

LIST OF TABLES

Table 1: Activity convertion factors 12

Table 2: Current depreciation during electroplating 25

Table 3: Radioactivity growth on working electrode 26

Table 4: Fraction transferred during electroplating 27

Table 5: Fraction transferred during arcing event 28

Table 6: Extraction summary (Experiment 1) 32

Table 7: Activity in aqueous extraction # 7 37

Table 8: Activity in aqueous extraction # 8 38

Table 9: Activity in aqueous extraction # 9 39

Table 10: Fraction activity extracted from malonate solution 46

Table 11 Distribution coefficient in malonate 47

Table 12: ^{221}Fr decay in aqueous extraction # 7 48

Table 13: ^{221}Fr decay in aqueous extraction # 9 48

Table 14: ^{221}Fr decay in aqueous extraction # 11 49

Table 15: ^{221}Fr decay in aqueous extraction # 13 49

LIST OF FIGURES

Figure 1: The synthesis of water soluble endohedral ^{225}Ac fullerene antibody complex .. 2

Figure 2 ^{225}Ac decaying products 4

Figure 3: Project overview 6

Figure 4: Bingel reaction 6

Figure 5: Electroplating set up 8

Figure 6: ^{229}Th decay chain 8

Figure 7: Efficiency curves 11

Figure 8: HPLC system 14

Figure 9: Air Brush for C_{60} deposition 16

Figure 10: Electroplating Set Up 17

Figure 11: Catcher 19

Figure 12: ^{225}Ac radioactivities on Pt electrode 26

Figure 13: Liquid-liquid extractions 29

Figure 14: Phase-activity distributions 30

Figure 15: Radioactivity in Organic phase 30

Figure 16: Summary of sequence of events 31

Figure 17: TLC radioanalyses of organic solution (Experiment 1) 33

Figure 18: ^{221}Fr decay in aqueous solution 36

Figure 19: HPLC spectra of empty C_{60} 40

Figure 20: HPLC spectra of 225Ac@C_{60} 41

Figure 21: HPLC spectra of malonate formation (step 1) 41

Figure 22: HPLC spectra of malonate formation (step 2) 42

Figure 23: HPLC spectra of malonate formation (step 3)..... 42

Figure 24: HPLC spectra of malonate formation (final step) 43

Figure 25: Extractions from malonate 44

Figure 26: Activity distribution 44

Figure 27: Partition coefficients Kd..... 45

Figure 28: ^{221}Fr decay in aqueous extractions 50

Figure 29: TLC spectra of malonate solution 50

Figure 30: TLC spectra of malonate solution (3 days later) 51

Figure 31: Escape mechanisms..... 55

Figure 32: ^{225}Ac background..... 57

CHAPTER 1

INTRODUCTION

1.1 Why C60 (fullerene)

Methods for linking β-emitting radionuclides to antibodies have been developed over the past decade, and the most recently Radio Immune Therapy (RIT) contains the β particle-emitters ^{90}Y and ^{131}I [1]. Different from β-particle-based therapy from α-particle-based therapy is that α-particle-based therapy offer much high cytotoxicity over a short range in tissue due to their greater linear energy transfer (LET) [2]. This property imparts α-particle with significant advantages over β-particle for therapies against single tumor cells and micrometatases [3]. Unfortunately, there are currently no sufficiently stable means for linking antibodies to the radionuclide such as ^{225}Ac that would otherwise be desirable for α-particle RIT [4]. Fullerene shows potential to contain α-emitting radionuclide. Fullerene with the truncated icosahedral structure (I_h) resembles a soccer ball, and contains hexagons and pentagons joined together in 6:6 ring bonds (between two hexagons) and 6:5 bonds (between hexagons and pentagons) [5]. The properties of C_{60} include: non toxicity, resistance to metabolism, a large carbon-based surface area, and a high kinetic stability [6]. The fullerene cage has an empty cavity large enough for complete encapsulation of atoms or small cluster of atoms. Therefore, radionuclide such as ^{225}Ac can potentially be encapsulated into the fullerene cage. The large carbon-based surface area of the fullerene cage can have a functional groups attached to it such as -COOH and -OH which make it to be water soluble molecule [7]. The derivatization of fullerene with malonate by the Bingle reaction leads to the formation fullerenemalonate compound which is soluble in organic solvents. Further treatment of this compound with CH_3OH leads to the cleavage of ester bonds in malonate to form fullerenemalonic acid which is soluble in the aqueous media. The Bingle cycloaddition reaction occurs at 6, 6-double bond and tends to reduce molecular angles strain by altering the hybridization of involved carbon i.e. from SP^2 to SP^3 [8]. Water soluble form is a prerequisite for the development of radiofullerene based therapy such as radio-endohedral fullerene antibody

conjugates. Therefore, for ^{225}Ac to be applicable for the therapeutical purpose, initially ^{225}Ac would be required to be encapsulated in C_{60} to form $^{225}Ac@C_{60}$. Secondly, $^{225}Ac@C_{60}$ would be converted to the water soluble form by treated with DBM followed by CH_3OH. Water soluble form ($^{225}Ac@C_{60}$*malonic acid) would allow the $^{225}Ac@C_{60}$ to be compatible with the in vivo environments. Theoretically, for the effective target treatment of affected cancer tissues, $^{225}Ac@C_{60}$*malonic acid would be required to conjugate with the antibody (Figure 1). Step by step synthesis of the conjugated complex follows 3 main stepladders; # 1 is the insertion of ^{225}Ac in C_{60} followed by surface chemistry modification, #2 is the tagging of antibody with organic linker to bridge with endohedral actinium fullerene (water soluble) as shown in step # 3. Briefly, because of their unique spherical structure, metallofullerenes offer a novel alternative method for entrapping radioisotopes and producing labeled compounds useful as radiotracers and for medical imaging and therapy.

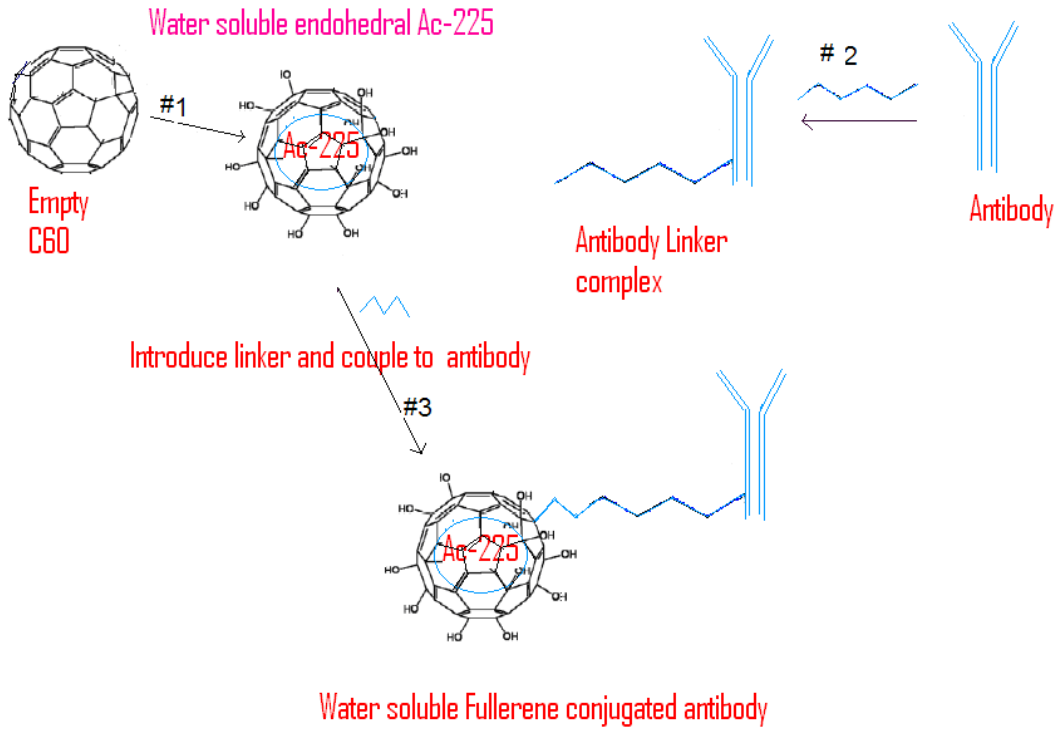

Figure 1: The synthesis of water soluble endohedral ^{225}Ac fullerene antibody complex

1.2 Why ^{225}Ac?

^{225}Ac is an alpha emitter radionuclide with a 10- day half life. The significant high linear energy released α particle from single parent radioisotope of ^{225}Ac, (Figure 2) and the characteristic half life of the nuclide, are among the features that make this radioisotope of interest in short range and site specific treatment of cancer diseases [9]. Both the speed and the mass of radioactive particles are important features for selection of radioisotope for the medical applications. In the beta particle-based therapy, beam of the beta particles is created outside a patient's body and directed at the tumor [10]. This therapeutical approach is made feasible as the results of the high penetrating power of high energy beta particles. The distinctive blending of low penetrating power and high specific ionization make alpha particles ideal for targeting cancer at the single cell level. The challenge is to develop a methodology for quick delivery to the targeted tissue. This is why fullerene chemistry was investigated for the possible application of providing delivery mechanisms for alpha emitter i.e. endohedral fullerene should provide a mechanisms for holding highly radiotoxic α – emitting isotopes such ^{225}Ac for which satisfactory conventional chelates do not exist. The α-particle that is released from the single decay event of ^{225}Ac travel approximately 50-70µm and deposits its energy in ~ 10 cell diameters. Therefore, in vivo ^{225}Ac can serve as an atomic scale generator for selective killing of targeted tumor cells [4]. For medicinal applications, ^{225}Ac and its decay daughters (francium-221, ^{221}Fr and bismuth-213, ^{213}Bi), needed to be completely chelated, otherwise the redistribution of ^{221}Fr and ^{213}Bi will add significantly to the non-targeted toxicity of ^{225}Ac.

1.3 Broad Spectrum

This thesis contains both the details of the first synthesis of endohedral actinium-225 fullerene ($^{225}Ac@C_{60}$) and the data on the molecular stability and attempt to improve its structure stability by the chemical modification method at the fullerene surface. The ^{225}Ac target was prepared through electroplating onto platinum electrode, and then subjected to a high potential-direct current electrical arc chamber for the insertion of

Radionuclide and Decay	Alpha Energy, E_α (MeV)	Recoil Energy, E_r (MeV)
^{225}Ac	5.75	0.10
10.0 d ↓ α		
^{221}Fr	6.36	0.12
4.8 m ↓ α		
^{217}At	7.07	0.11
32 ms ↓ α		
^{213}Bi 45.6 m	5.8	0.10

Figure 2 ^{225}Ac decaying products

^{225}Ac into the fullerene cavity to form ^{225}Ac@C_{60}. The endohedral ^{225}Ac @C_{60} in toluene solution was washed six times to extract un-encapsulated radionuclide (Figure 3). During the course of extractions, fullerene complex structure was observed to dissociate chemically and released the radioisotope into the aqueous media. The chemical dissociation was triggered by both process; the nuclear recoil reaction and the mechanical forces exerted on the carbon ring frame work. The energy associated with the momentum conservation from the nuclear dissociation event was high enough to disrupt the cage structure of the complex and discharged the radionuclide. The SP^2 hybrid carbon in empty C_{60} was a high energy conformation. Therefore, the bond angle that was formed associated with the double bonded carbon resulted in high molecular strain structure [11]. The data analysis suggests that, the insertion of ^{225}Ac into C_{60} creates more strain onto the fullerene frame work, which eventually collapses to a low energy conformation.

An effort to improve structure stability of the ^{225}Ac@C_{60} was attempted using Bingel nucleophilic cycloaddition reaction (Figure 4). The extent of the reaction completion between malonic ester and C_{60} at the fullerene surface was monitored by means of HPLC. The synthesis of the endohedral conjugated malonate derivative was achieved by refluxing the solution mixture that contains ^{225}Ac @ C_{60}, toluene and diethyl bromomalonate (DBM) in basic medium. The HPLC with bucky prep column was used for successfully separation between ^{225}Ac @ C_{60} malonate complex and ^{225}Ac @ $C_{60.}$ The surface chemistry of the modified conjugated endohedral fullerene serves two main purposes: Firstly, provides a medium in which endohedral ^{225}Ac@C_{60} complex is converted to a water soluble form. The solubility property of the complex is very crucial for both possible medical applications as well as for in vivo studies. Secondly, provides the enhancement of structure stability against chemical dissociation effects.

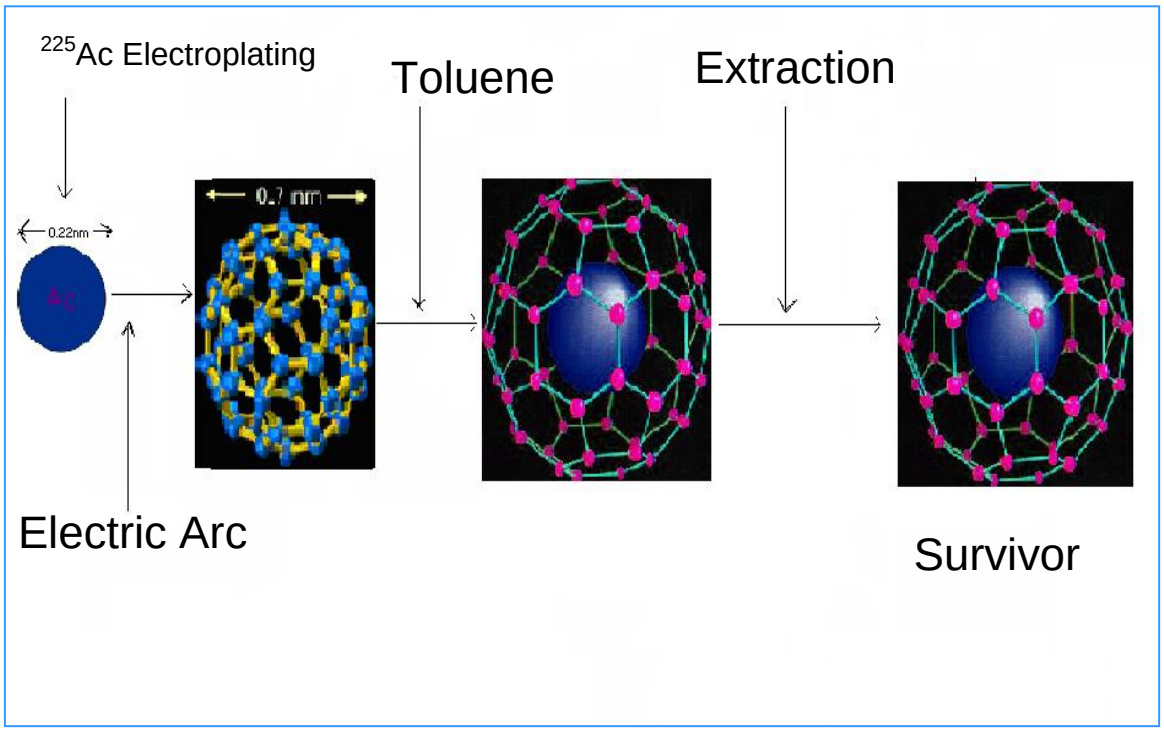

Figure 3: Project overview

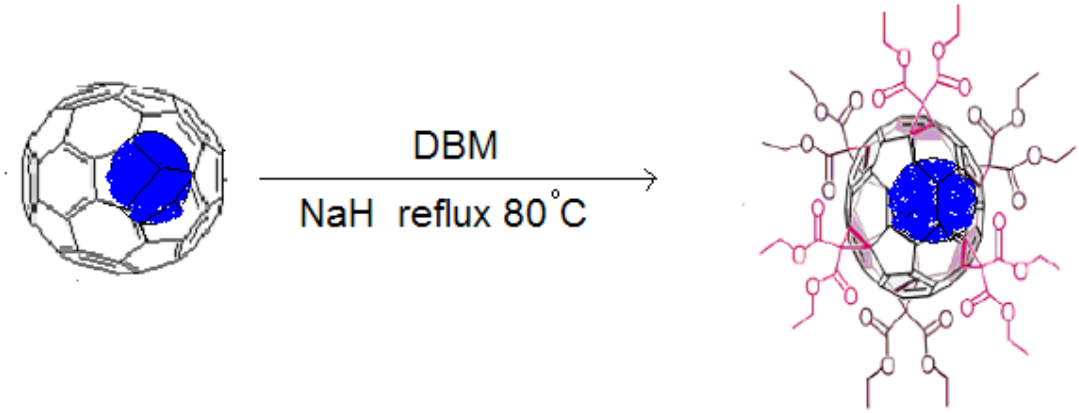

Figure 4: Bingel reaction

CHAPTER 2

EXPERIMENTAL

2.1 Materials and chemicals

The electroplating set up (Figure 5) was composed of two circular Pt electrodes with the dimensions of 1cm diameter and 1mm thick. The electrode on the left was used for deposition of ^{225}Ac. It was attached to a 6 cm Pt wire which was encased in a glass tube. The counter electrode, unlike the deposition electrode, was made of Pt mesh, and attached to a 6cm wire which was also encased in a glass tube. Fullerene C_{60} (99%) from Sigma Aldrich and TDA Research Inc was used without further purification. Nitric acid HNO_3 from EM Science and tetrahydrofuran (THF) from Sigma Aldrich were used as received. Diethylbromomalonate (DBM), HPLC grade toluene, and sodium hydride (NaH) were purchased from Sigma Aldrich and used without further distillation. A 1 – 2 mCi quantity of ^{225}Ac from the Nuclear Medicine Program at Oak-Ridge National Laboratory was used for each electroplating operation. An artist's air brush (Airbrush City Inc Model # 2084427450) was used for applying a thin coat of C_{60} to Al disks. A direct current power supply (high potential – low current direct current) Hewlett Packard 6205C model was used for electric arcing between C_{60} catcher disk electrodes and the ^{225}Ac deposited electrodes under He atmosphere. A low potential-low current D.C power supply (459 ORTEC) was used for electroplating ^{225}Ac onto Pt electrodes.

2.2 Production of ^{225}Ac

^{225}Ac is currently obtained from the thorium -229 (^{229}Th) decay chain (Figure 6). The actinium - 225 (^{225}Ac) was produced as reported in Boll et al. Appl.Radiat.Isot.62 (2005)667. In brief, carrier free ^{225} Ac was separated from a mixture that contained ^{228}Th, ^{229}Th, and ^{225}Ra through a sequence of chemical steps which employed both anion and cation exchange column chromatography. Macroporous anion exchange resin (MP1) in

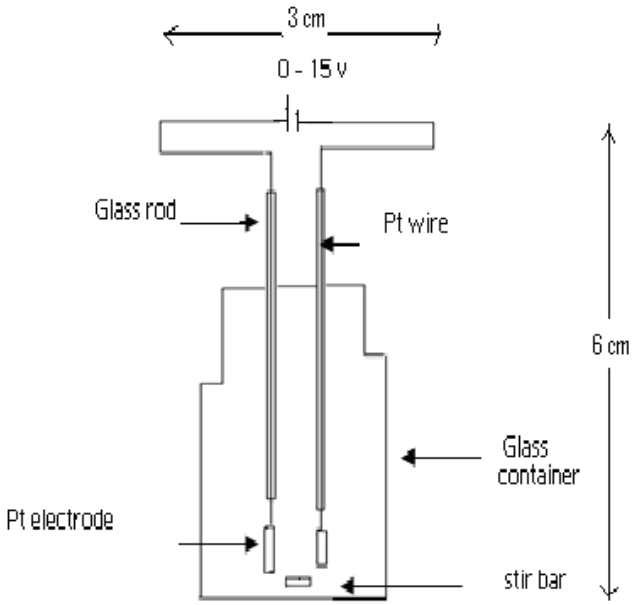

Figure 5: Electroplating set up

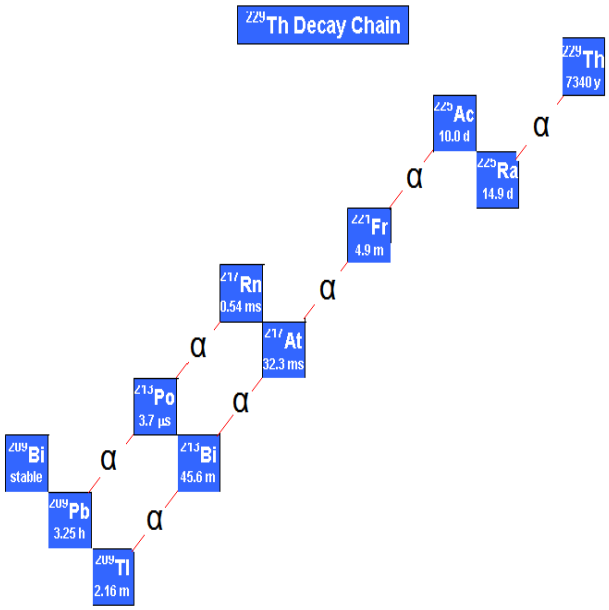

Figure 6: ^{229}Th decay chain

HNO_3 was used to separate ^{225}Ac and radium - 225 (^{225}Ra) from the thorium isotopes. Low cross-linked cation exchange resin (AG 50-X4) in HNO_3 solution was used to separate actinium from the bulk solution that contained radium, see figure 7. Typically carrier free ^{225}Ac (1 – 2 mCi in 100 – 200 µL) was transferred to an electrolysis cell and evaporated to dryness. The invisible radioactivity was then dissolved in 10 ml of 0.01 M HNO_3 ready for the electrodeposition process.

2.3 Radioactivity Measurements

The radioactivity measurements of all isotopes that were involved in this project were made using gamma-ray spectrometry. The spectrometer consisted of a calibrated intrinsic Ge detector (crystal active volume ~100 cm^3) interfaced to the PC-based multichannel analyzer (MCA) (Canberra Industries, Meriden, CT). The resolution of the detector was 0.8 keV at 5.9 keV, 1.0 keV at 123 keV and 1.9 keV at 1332 keV. Energy and efficiency calibrations were determined with Standard γ-ray sources traceable to the National Institute of Standard and Technology (NIST).The energies of γ-rays and absolute intensities I_γ (in parenthesis) of ^{225}Ac, ^{221}Fr, and ^{213}Bi radioactivity were 188 keV (.47%), 218 keV (11.58%), and 440 keV (26.1%), respectively. The instrument was initially calibrated before use, and the efficiency curves for shelves 2 cm through 60 cm for ^{225}Ra, ^{225}Ac, ^{221}Fr, and ^{213}Bi were obtained (Figure 7). The radioactivity conversion factors for ^{225}Ra, ^{225}Ac, ^{221}Fr, and ^{213}Bi i.e. the radioactivity conversion from counts per seconds to microcuries were computed and recorded in Table 1 (cps/factor = µCi). Due to the natural behavior of ^{225}Ac of having a γ-ray with weak intensity of (0.47%), the γ-ray of its decay daughter ^{221}Fr (11.58%), was frequently used to monitor and quantify the activities of ^{225}Ac. Accordingly, 30 min were allowed between the end of chemical operations and radioactivity assay for ^{221}Fr to reach 99% equilibrium with ^{225}Ac. All relevant nuclear data were taken from the Atomic Data and Nuclear Data Tables, Vol.29, No.2, September1983. In addition to gamma-ray spectrometry, the ionization chamber (CRC-7,

Capintec Inc., NJ), was used for gross measurements of higher levels of radioactivity. The chamber was calibrated against Gamma ray spectrometer before use.

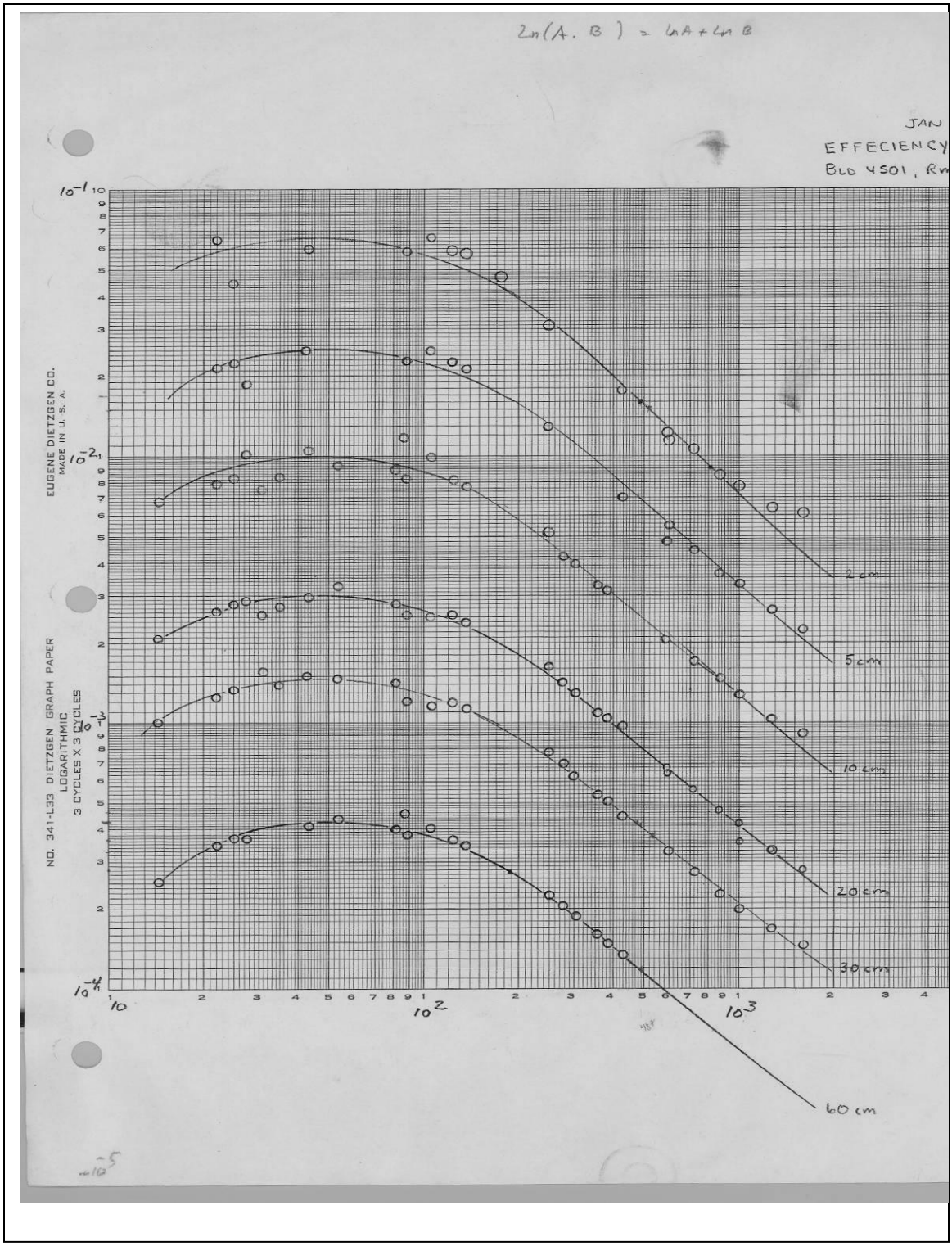

Figure 7: Efficiency curves

Table 1: Activity convertion factors

SHELF 60				
Nuclide	**Energy (kev)**	**I_γ (%)**	**Efficiency**	**Factor**
Ra-225	40.3	30	4.30 E-4	4.77
Ac-225	188	0.47	2.80 E-4	0.048
Fr-221	217	11.6	2.45 E-4	1.05
Bi-213	440	26.1	1.40 E-4	1.325
SHELF 30				
Ra-225	40.3	30	1.48 E-3	16.4
Ac-225	188	0.47	9.40E-4	0.16
Fr-221	217	11.6	8.20E-4	3.51
Bi-213	440	26.1	4.40E-4	4.25
SHELF 10				
Ra-225	40.3	30	9.0E-3	99.9
Ac-225	188	0.47	5.9E-3	0.96
Fr-221	217	11.6	5.3E-3	22.7
Bi-213	440	26.1	2.7E-3	26.1
SHELF 5				
Ra-225	40.3	30	2.6E-2	288
Ac-225	188	0.47	1.7E-2	2.95
Fr-221	217	11.6	1.5E-2	63.4
Bi-213	440	26.1	7.4E-3	71.5

2.4 Thin Layer Chromatography-Biocanner

A radioactivity imaging scanner System 200-IBM with an auto-changer (Bioscan, Inc Ar-2000), equipped with Winscan Software Version 2.2 for the instrumental control and data acquisitions was used for the TLC radioanalyses. This analytical tool allows a direct counting of the radioactivity presented on developed TLC plates. In a single run, a 20 to 25 min period was required for the TLC plate that contained a sample of solutions of ^{225}Ac, C_{60}, C_{60}*malonate, $^{225}Ac@C_{60}$ and $^{225}Ac@C_{60}$*malonate to be developed in organic solvents and assayed for radioactivity. This time period was enough for 90% (roughly) equilibrium growth of ^{221}Fr from ^{225}Ac. Normally, each developed plate was continuously assayed for radioactivity over three consecutive days to characterize the isotopic peaks. Based on the peak intensity depreciation rate as the function of time, the successive analyses of the same plate would suggest the possible half lives of the nuclides present in that particular plate. To pin point that a particular peak corresponded to ^{213}Bi (t ½ = 45.6 min), the TLC plate was subjected to analyses at 3 hour time intervals. The peaks that were observed to decay with a characteristic half- life of 45.6 min, confirmed the presence of ^{213}Bi. However, in this time window, the peaks intensity that were observed to remain unchanged, suggested the presence of ^{225}Ac (t ½ = 10 d). In order to identify the peaks that corresponded to ^{221}Fr (t ½ = 4.8 min), TLC plates were subjected to short time analyses of 2 min intervals for a period of 20 min. Several TLC-based control experiments were initially carried out. These consisted of career- free ^{225}Ac, C_{60}, malonic ester, $^{225}Ac@C_{60}$ and $^{225}Ac@C_{60}$*malonate, and they were developed as follows. (1) Standard TLC plates of carrier- free ^{225}Ac in HNO_3 were developed against ethyl acetate**.** (2) Standard TLC plates of carrier - free ^{225}Ac in HNO_3 were developed against toluene. (3) Standard TLC plates of a heterogeneous mixture of fullerene and malonic ester in toluene solution were developed against ethyl acetate**.** (4) Standard TLC plates of ^{225}Ac $@C_{60}$ in toluene solution were developed against toluene.(5) Standard TLC plates of ^{225}Ac $@C_{60}$*malonic ester were developed against ethyl acetate. The results and the discussions on these plates can be found in Chapter 3 of this thesis.

2.5 High Performance Liquid Chromatography (HPLC)

A HPLC instrument equipped with a millennium work station, flow splitter and high pressure 515 pumps with a keypad, and LCD display for quick readout and parameter control was used. This analytical tool (Figure 8), with the detection system (996 PDA online UV) and a cosmosil bucky prep analytical column (code # 379-81, size 10 × 200mm) was useful for separations and identifications of fullerene, endohedral ^{225}Ac fullerene and endohedral ^{225}Ac fullerene malonate complex . The organic samples were initially dissolved in toluene and filtered before use. During processing, a 5 µL sample volume was injected each time using 10 µL syringes. The system was performed under isocratic conditions with toluene as a mobile phase. The millennium work station was used to achieve quick and reproducible acquisitions and characterizations of fullerene and its derivatives. The HPLC spectra and retention time of the empty fullerene in toluene solution were collected and then subjected to comparisons with the experimental spectra, mainly ^{225}Ac @C_{60} (in toluene) and ^{225}Ac @C_{60}*malonic ester (in toluene) . The column was flushed with a mobile phase each time before injection for complete removal of contaminants.

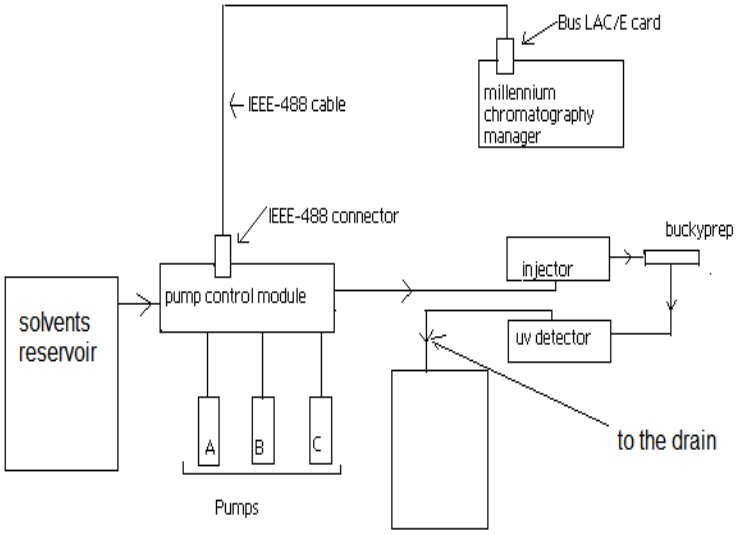

Figure 8: HPLC system

2.6 Mass Spectrometry

Mass spectrometry played a big role in the discovery of fullerenes and related compounds (G. Rong Her et al. 1995). Varieties of mass spectrometric ionization techniques have been used for the characterization of fullerenes and its derivatives (A. Herod et al. J. Chem. Soc. Perkin Trans.2 1994). These include electron impact, chemical ionization, desorption chemical ionization, fast-atom bombardment, laser desorption and matrix-assisted laser desorption ionization (MALDI), (V. Kozlovski et al. 2004). It has been reported by L. Michalak et al.2003 and H. Shinora et al 1992 that many of fullerenes and related compounds were fragile. Therefore, these compounds tend to experience chemical degradations during ionization. As a result of this phenomenon of molecular degradation, it becomes difficult to obtain clean spectra with a single peak as a molecular ion signal of the analyte. An ideal ionization technique would be the one that produces only the molecular ions with little or no fragmentation. In the ESI mass spectrometer, an electrical charge is used to assist the transfer of ions from the solution into the gas phase at atmospheric pressure conditions (Principle of instrumental analysis by D. Skoog 5th edition, 1998, pg 498). During the course of this project, electron spray ionization (ESI) mass spectrometry was used as a source of soft ionization and subsequent characterization of the fullerene and fullerene malonate. Endohedral ^{225}Ac @C_{60} and endohedral ^{225}Ac@C_{60}*malonate were not analyzed by mass spectrometer for 3 main reasons: (1) low yield of ^{225}Ac @C_{60} below the range of the detection limit of mass spectrometry, (2) inability of the ^{225}Ac @C_{60} to be purified from the starting material (empty fullerene), and (3) due to its radioactivity, we were forbidden to inject it into the mass spectrometer. In order to validate the methodology that an atom or clusters of small atoms could be inserted in a C_{60} cavity through an electric arc in He atmosphere, the experiment was repeated using cold gadolinium (Gd) metal. A concentrated Gd solution in HNO_3 was prepared and then subjected to the same treatment as in the ^{225}Ac in order to synthesize Gd @ C_{60}. The organic solution that suspected to contain Gd@C_{60} was digested with H_2O_2 then submitted for Inductive Couple Plasma (ICP) mass analyses. The results indicate that Gd was present.

2.7 Artists Air Brush

An Artists Air Brush (Airbrush City Inc. model # 2084427450) was used for the preparation of a thin coat of C_{60} on an aluminum (Al) disk (Figure 9). The container was used for holding a fullerene solution in toluene and a plastic pipe was connected to the air tank to generate pressure for solution mobility. The amount of air supply and the solution spray rate were controlled by means of a valve. Normally, a super saturated solution of fullerene (C_{60}) was prepared by dissolving 1 g of C_{60} in 10 mL of toluene. Then, using the Artist Air Brush, C_{60} solution was sprayed onto an Al disk while the disk was placed on a hot plate kept at the lowest temperature setting. The process was repeated several times until 1.5- 2.0 mg of C_{60} were deposited to form a relatively uniform layer.

Figure 9: Air Brush for C_{60} deposition

2.8 Electroplating

The electroplating cell (Figure 10), of conventional design, consisted of a 20- mL scintillation vial, and working electrode and counter electrode. A Hewlett Packard 6205C D.C Power Supply was used to maintain a constant potential bias between electrodes. The circuit configuration was such that the electrode to be platted was attached to the negative potential terminal of the power supply and the positive terminal was directly connected to the counter electrode. The flow of charge throughout the electrodeposition circuit was completed by a solution of dilute HNO_3. The chemical decomposition of the electrolyte as current was passing through caused a significant increase in the solution temperature which led to solution evaporation. In order to maintain a constant electrolytic volume, additions of dilute acid were carried out as electroplating was in progress.

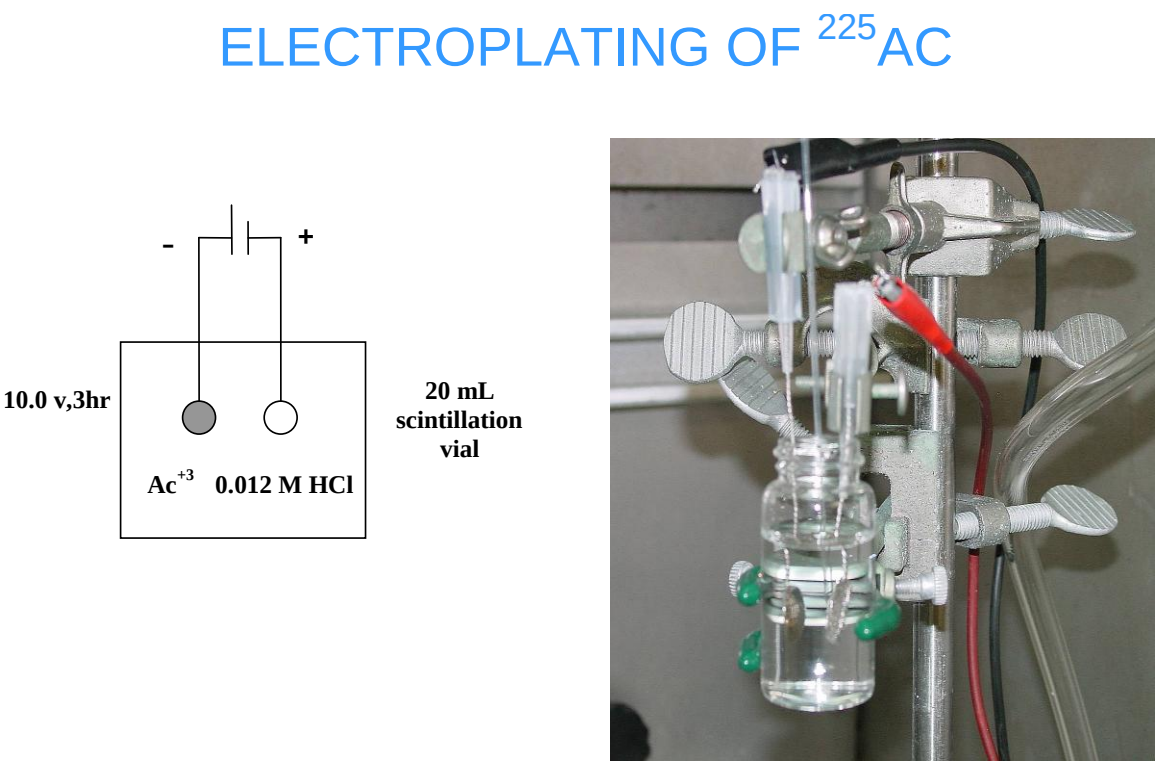

Figure 10: Electroplating Set Up

2.9 Recoil Catcher Apparatus / Arc Chamber

The recoil catcher apparatus / arc chamber consisted of two glass pieces that were attached together through a flat joint. The chamber has a helium (He) inlet valve and an outlet valve located on the opposite side of the apparatus. The glass capillary 6 cm O.D and 1 mm I.D located 2 cm from the flat joint serve the purpose of supporting the working electrode. The C_{60} catcher was coupled to a metal rod by means of screw (Figure 11). The metal rod serves two purposes: (1) It provides the mechanism to suspend the C_{60} catcher disk inside the chamber and (2) it serves as a electrical conductor during the arcing. Low pressure He gas was allowed to leak into the chamber with just enough flow rate to support the arcing. The working electrode could be moved in a vertical direction and the catcher disk in a lateral direction. The movements of the electrodes were made possible by sliding the appropriate rods through the indicated O – rings. Vacuum seal and gum like materials were used to minimize He leaks. Normally, at the initial steps of arcing, small amounts of fullerene fell. This was from the Al catcher disk as a result of the intense activity between the electrodes.

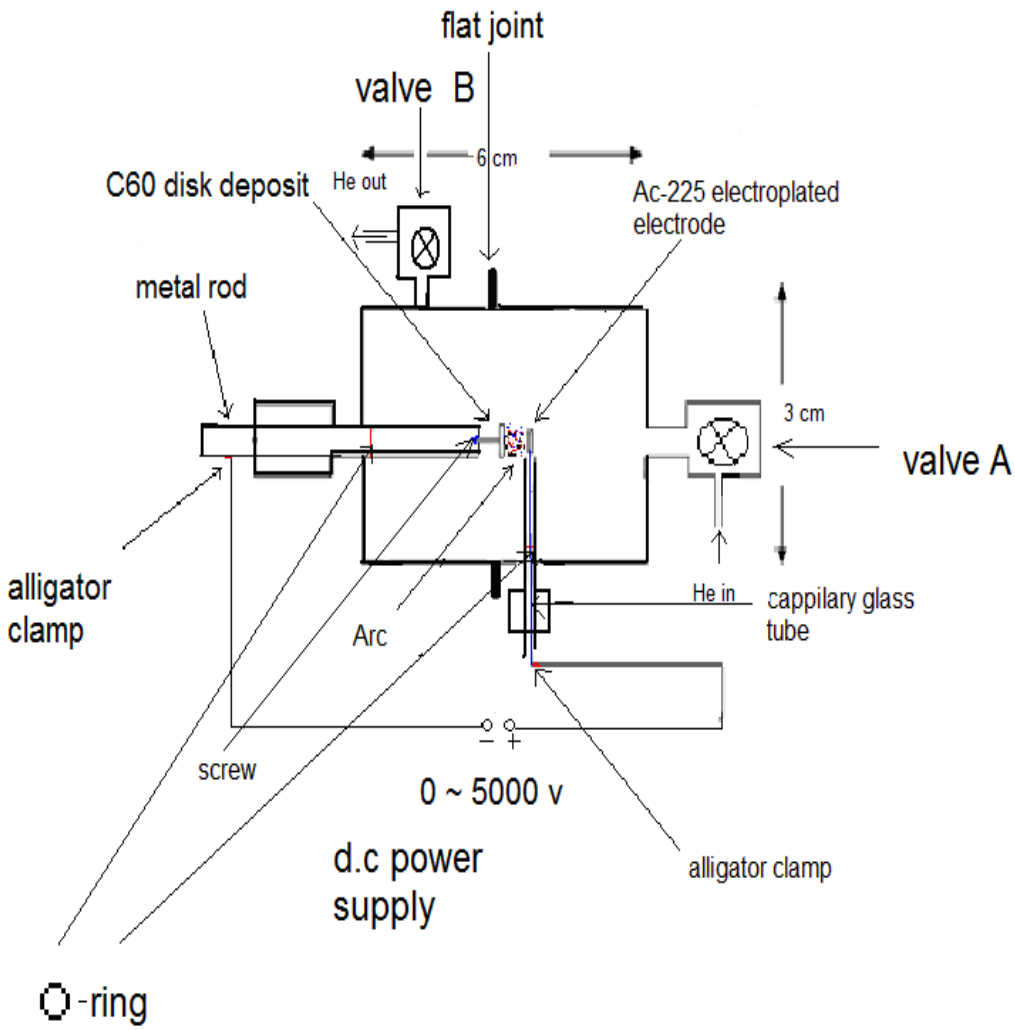

Figure 11: Catcher

CHAPTER 3

EXPERIMENTAL PROCEDURE

3.1 Fullerene Catcher Disk

A thin layer of fullerenes deposited on Al disks was achieved by an artistic air brush method. This approach, as it has been described in section 2.7, is proven to be a reliable technique. In each deposition over 1 mg of C_{60} was firmly attached to the metallic surface. The process was initiated by preparing a super-saturated solution of C_{60} in toluene. The solution was then transferred to a container which was connected to an air brush apparatus. A moderate flow-rate of air created a highly volatile mixture. This mixture was then projected onto the surface of an Al disk which was positioned on a hot plate to evaporate the solvent as it was deposited.

3.2 Process for Electroplating of ^{225}Ac

The electrolysis cell that was described earlier in chapter 1, was operated using a 10 -11 V fixed potential and a current of 1.56 -1.80 A. Normally, the electrolytic solution was made up of 1-1.5 mCi of ^{225}Ac in 10 ml of 1.2 M HNO_3. These initial operating conditions were found to be optimum for the electroplating of ^{225}Ac onto the Pt electrode. The electrolytic solution was prepared by taking a source solution of ^{225}Ac in 1 mL of dilute acid in a vial, and was evaporated to dryness on a hot plate. The invisible deposit of ^{225}Ac radioactivity was allowed to cool and 10 mL of 0.01 M HNO_3 was added to the cell to dissolve it. The solution was then transferred to a 20-mL scintillation-vial electroplating cell. The working electrode, counter electrode, and the magnetic stir bar were then introduced into the electroplating cell. The working electrode (in disk form) was connected to a negative terminal while a counter electrode (mesh like) was connected to the positive terminal, both by means of alligator clamps. The rate of

electroplating was monitored by withdrawing 100 µL aliquots at 1 hr intervals and analyzing them for radioactivity. At the conclusion of the electroplating, the working electrode was removed from the solution while the potential was still maintained. This prevented the electroplated ^{225}Ac from redissolving into the solution. On average, over 70 % of ^{225}Ac was electroplated in each trial.

3.3 Procedure for the Insertion of ^{225}Ac into C_{60} via Electrical Arc

Initially, the two parts of the arc chamber were separated at the flat joint, and the C_{60} catcher disk was inserted and tightly coupled to the metal rod by means of a screw. The ^{225}Ac- plated Pt electrode was then inserted into the chamber. Vacuum grease was used on the flat joint to suppress He leaks. The chamber was closed and flushed with He, which flowed into the chamber through valve A and out through valve B. The positive and negative terminals of the power supply (ORTEC model # 459 D.C) were connected to the working electrode (+ve) and the metal-rod catcher disk (-ve) respectively. A constant potential of 4000 V-4500 V (low current $\leq$ 5 mA) was used to generate an electrical arc between the two electrodes. The need for such a high potential was caused by the insulating layer of C_{60}. He gas was allowed to leak continuously into the recoil catcher apparatus, since experiments demonstrated that this was the best atmosphere for the arcing. The electric arc was maintained for 2 hrs. During this period the ^{225}Ac-Pt electrode was manually maneuvered (front to back and up and down) to make certain that the arc struck different positions of the electrode surface. After 2 hours, the power supply and He flow were turned off. The arc chamber was then opened and the C_{60} catcher disk was removed and then transferred to a clean container where it was assayed for radioactivity. Once there was evidence of enough radioactivity on the C_{60} catcher disk, then the ^{225}Ac-C_{60} catcher disk was immersed in 5 mL toluene solution for 5 minutes to form a purple-colored solution. This step was performed purposely to extract materials that were easily soluble in the organic solvent. The disk was then removed from the solution and transferred to a clean empty container.

3.4 Procedure for the Extraction of ^{225}Ac from the Organic Phase

The purple colored organic solution acquired earlier (section 3.5), was assayed for radioactivity and found to contain ^{225}Ac. The solution was then subjected to a series of extraction processes. The toluene solution was brought in contact with 5 mL of 0.01 M aqueous HNO_3 to form an immiscible two-phase system. This system was intended to extract water-soluble radionuclides from the organic solution**.** The solution mixture was shaken for 1-2 min and allowed to settle. Using a volumetric pipette, the aqueous layer was carefully removed and transferred to a clean vial. The aqueous solution was then back washed using 1 mL of toluene to extract any organic portion that may have escaped during separation. The above-mentioned process of separation and back washing was repeated 6 times using fresh 5 mL portions of 0.01 M HNO_3 and fresh 1 mL portions of toluene for the back wash. All phases were assayed for radioactivity.

3.5 Procedure to Investigate the Fate of ^{221}Fr upon Decay of $^{225}Ac@C_{60}$.

The nuclear dissociation event in which ^{225}Ac decays to its daughter nucleus, ^{221}Fr, was investigated. As the result of a liquid-liquid extraction (section 3.4), the source of ^{225}Ac in the aqueous phases could be: (a) ^{225}Ac was not incorporated in the C_{60}, (b) ^{225}Ac was incorporated in the C_{60}, and then escaped by disrupting the cage. The source of the ^{221}Fr could be: (1) the ^{221}Fr came from the decay of ^{225}Ac which had not been incorporated in the C_{60}, (2) the ^{221}Fr came from the ^{225}Ac incorporated in the cage which then escaped from the cage, (3) the ^{221}Fr came from ^{225}Ac incorporated in the cage and the decay recoil drove it through the cage. To distinguish the pathway (2) from pathway (3) the organic solution (section 3.4) was left undisturbed for at least 30 min. This allows growth of ^{221}Fr to reach 99% equilibrium with ^{225}Ac. Further extraction was performed (totaling seven extractions) and analyzed for a short time specifically for ^{221}Fr counts. The decay of ^{221}Fr was followed for over 20 minutes until the equilibrium between ^{221}Fr and ^{225}Ac was attained. The remaining organic solution was equilibrated over night and assayed for radioactivity the following day. Using the same acidic concentration and volume, two

additional extractions (totaling nine) were performed in 30 minute time intervals. The left over organic solution was characterized by HPLC and TLC- radioanalyses. The evidence of ^{221}Fr in the extracted aqueous phase suggested that mechanism (3) occurred.

3.6 Procedure for Fullerene Surface Modification

The organic solution was further investigated and it was determined that the $^{225}Ac@C_{60}$ was unstable. A new procedure was introduced to examine the possibility of enhancing molecular stability. The organic solution (section 3.5) was transferred to a two-neck shaped flask. The toluene was removed under N_2 and a mixture of 0.02 mL of DBM and 4 mL of THF containing 3 mg of suspended NaH were added. The THF slurry was transferred by syringe from the flask into a 15-mL polypropylene conical-bottom centrifuge tube. The mixture was centrifuged to separate the sediment of sodium salt from the solution. The supernatant was transferred to a clean three-neck flask and evaporated to dryness under N_2. One mL of DBM and 10 mL of toluene containing 3 mg of suspended NaH were added. The solution was refluxed at 80^0C for 6 hrs while it was purged with N_2. The solution color was observed to change from dark-purple (color of fullerene) to reddish, as the fullerene malonic ester was being formed. The extent of reaction completion was monitored by HPLC. This was made possible by withdrawing 5 µL aliquots from the reaction mixture and analyzing them with HPLC.

3.7 Removal of Exohedral ^{225}Ac

The fullerene malonate solution (section 3.6) was contacted with diluted acid to remove all radionuclides that were soluble in the aqueous media. Fresh aqueous solution containing 10 mL of 0.01M nitric acid was added to the 10 mL fullerene malonate solution in a 40 mL glass vial. The mixture was shaken for 1 to 2 minutes and then allowed to settle for 30 seconds. Using a volumetric pipette the aqueous layer was carefully removed and transferred to a clean vial (section 3.4). This solution was then back washed with 1 mL of toluene to extract the radioactivity that might have migrated to

the aqueous solution during phase separation. The process was repeated five times. The organic layer and aqueous washes were then assayed for radioactivity.

CHAPTER 4

RESULTS

4.1 Electroplating

The preparation of thin layer of alpha source-target such as ^{225}Ac has been already reported by Shinohara et al. [6, 7, and 8]. Electroplating of ^{225}Ac onto a Pt electrode was a step towards the synthesis of $^{225}Ac@C_{60}$. During electroplating, the current was dropped as the process was in progress, Table 2. The working electrode was monitored by radioanalyses (Table 3 and Figure 12) to determine how stable was ^{225}Ac plated on Pt electrode. The growth of the radioactivity that eventually equilibrated to a single value justify that ^{225}Ac on Pt was a stable source.

Table 2: Current depreciation during electroplating

Real time (pm)	Voltmeter reading	Ammeter reading
4:34	10.17	1.37
4:51	10.16	0.74
4:57	10.16	0.61
5:26	10.16	0.57
5:30	10.16	0.52
5:37	10.16	0.49

Table 3: Radioactivity growth on working electrode

Real time (pm)	Radioactivity (µCi)
12:55	677
01:04	775
01:11	837
01:34	982
01:49	1050
01:55	1070

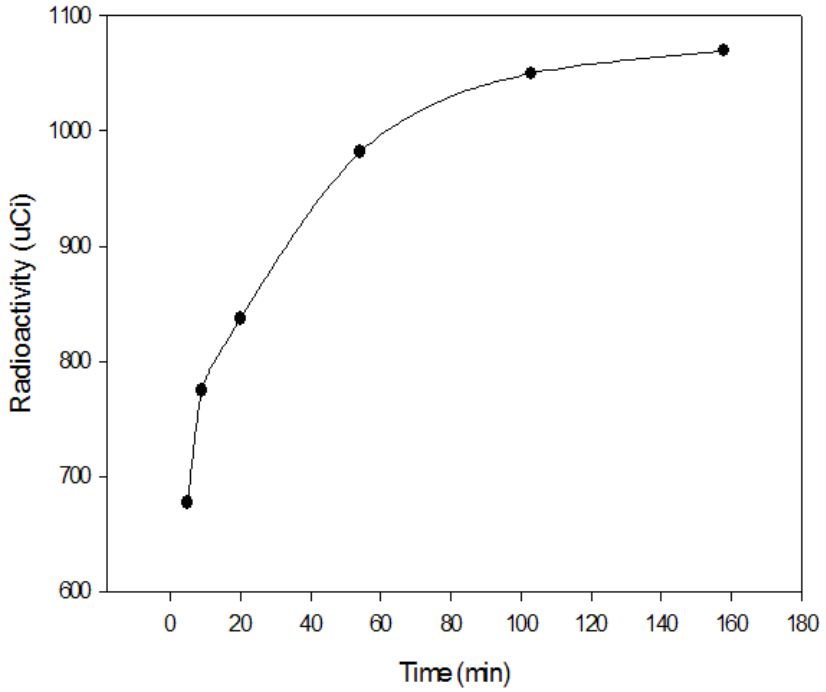

Figure 12: ^{225}Ac radioactivities on Pt electrode

In general, over 70% of ^{225}Ac was electroplated (Table 4). It has been reported that physical factors such as solution temperature, electrode gap and electrode rotation, pH of the supporting electrolyte, solution concentrations, and cell potential influence the extent of ^{225}Ac to be plated [12,13]. In this project, attempts to study the effects of these factors were not investigated. The amount (> 70%) was found to be enough to carry out the electric arc experiment. Through the course of this investigation over 20 arcing experiments were carried out. Table 5 is an example of experimental results, which illustrates the randomness of the arcing system. Assays of the radioactivity on the C_{60} catcher disk indicate trace amounts of ^{225}Ac. On the first experiment, 12% (48 cps) of ^{225}Ac was initially transferred to the C_{60} catcher disk. This amount was allowed to decay for 3 days, and then was increased by 5 counts when the second arc was applied. Changes in ^{225}Ac counts on the fullerene catcher disk during each arcing cycle suggest that further study is necessary for better understanding of the fundamentals that govern this deposition.

Table 4: Fraction transferred during electroplating

Experiment #	Description	^{225}Ac radioactivity (cps)	% Fraction electroplated
1	Initial radioactivity in solution	740	0
	^{225}Ac radioactivity electroplated	556	75
2	Initial radioactivity in solution	496	0
	^{225}Ac radioactivity electroplated	396	80

Table 5: Fraction transferred during arcing event

Experiment #	Event	^{225}Ac (cps)	% Activity
1	Electroplated ^{225}Ac (day 1) Electroplated ^{225}Ac (day 3)	415 367	100
	^{225}Ac on C_{60} disk # 1-1st arc(day 1) ^{225}Ac on C_{60} disk # 1- (day 3)	48 39	12
	^{225}Ac C_{60} disk # 1-2nd Arc(day 3)	44	13
2	Electroplated ^{225}Ac source (day 1)	320	100
	^{225}Ac on C_{60} disk #2 -1st Arc (day 1)	3	1
	^{225}Ac C_{60} disk # 2 -2nd Arc (day 4 later)	11	5

4.2 Extractions

Successive liquid-liquid extractions into dilute HNO_3 (Figure13) followed by radioanalyses of both phases, (Table 6) illustrated that more than 80% of ^{225}Ac ($^{221}Fr/^{213}Bi$ counts) was initially extracted. This implies that repeated washing of the organic phase with nitric acid removed most of radionuclides that were water-soluble. The outcome also verifies that subsequent to six extractions of the organic phase some of ^{225}Ac was still retained. The radioactivity distributions in both organic and aqueous phases, exhibited a well-established francium/bismuth equilibrium, which proved that the parent ^{225}Ac was present (Figure 14). All this together demonstrated that (1) some of ^{225}Ac could not be extracted from the organic phase and (2) was apparently inside the fullerene (Figure 15). The sequence of events that led to the synthesis of $^{225}Ac@C_{60}$ could be summarized as in Figure 16.

Figure 13: Liquid-liquid extractions

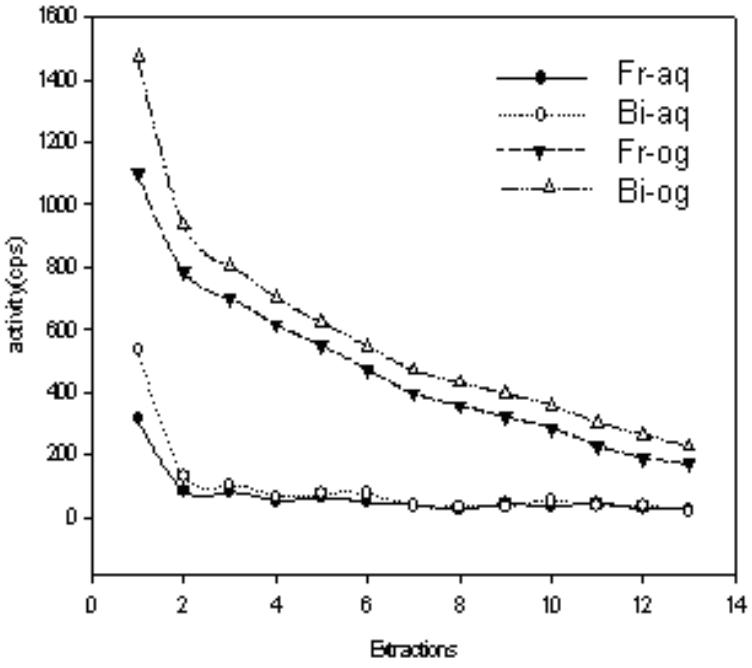

Figure 14: Phase-activity distributions

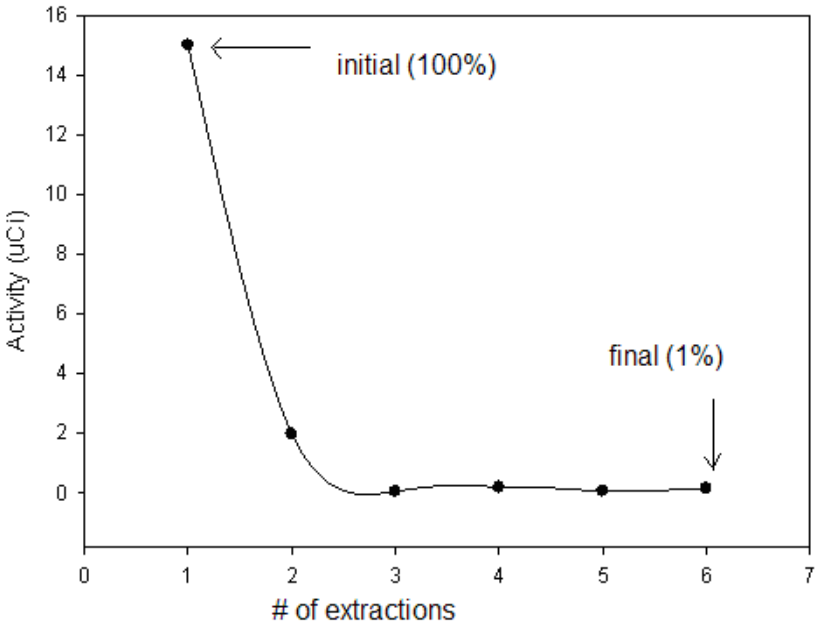

Figure 15: Radioactivity in Organic phase

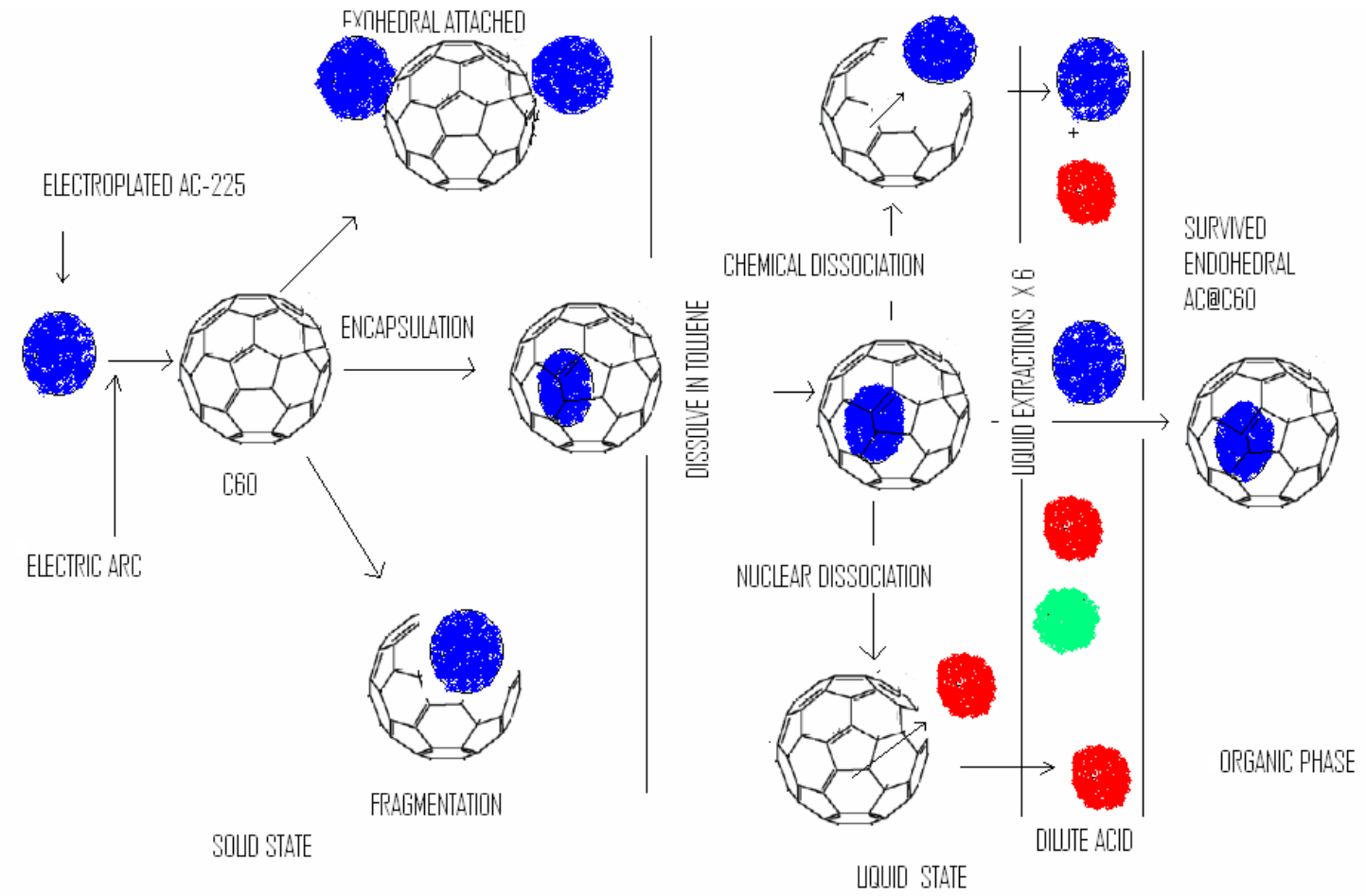

Figure 16: Summary of sequence of events

Table 6: Extraction summary (Experiment 1)

Date	Time	Event	Assay of Radioactivity						
			AT	SF	Fr 221				
					Total Counts	% error	cps	uCi % activity	% Extracted activity
11/18/2006	2:17	1ml of 10ml initial Organic solution	5	5	11100	1.22	36 9	18	100
11/18/2006	2:24	Extraction AQ # 1	3	30	9490	1.25	52.7	15.0	82
11/18/2006	2:28	Extraction AQ #2	3	30	1250	3.39	6.95	1.98	11
11/18/06	2:32	Extraction AQ #3	3	30	355	7.12	1.97	0.56	3
11/18/2006	2:35	Extraction AQ # 4	3	30	122	10.6	0.67	0.19	1
11/18/2006	2:39	Extraction AQ # 5	4	30	56.2	18	.259	0.074	.4
11/18/2006	2:53	Extraction AQ # 6	2	5	1230	3.4	10.2	0.16	.87

AT = analysis time, SF = shelf position, TC = total counts

4.3 Chromatography

The radioanalyses of the organic solutions using TLC revealed that the ^{225}Ac radioactivity remained at the origin and the C_{60} moved with the solvent front (Figure 17). The partition distribution of ^{225}Ac between toluene and nitric acid (Table 7) illustrate that most of ^{225}Ac exist in an ionic form. The radioanalyses of aqueous phases extraction number seven (Table 7) and (Figure 18), and aqueous extractions number eight and nine (Table 8 and 9), illustrated that ^{221}Fr activity (cps) remained almost unchanged suggested the company of the ^{225}Ac. This confirms that ^{225}Ac escaped from the cage.

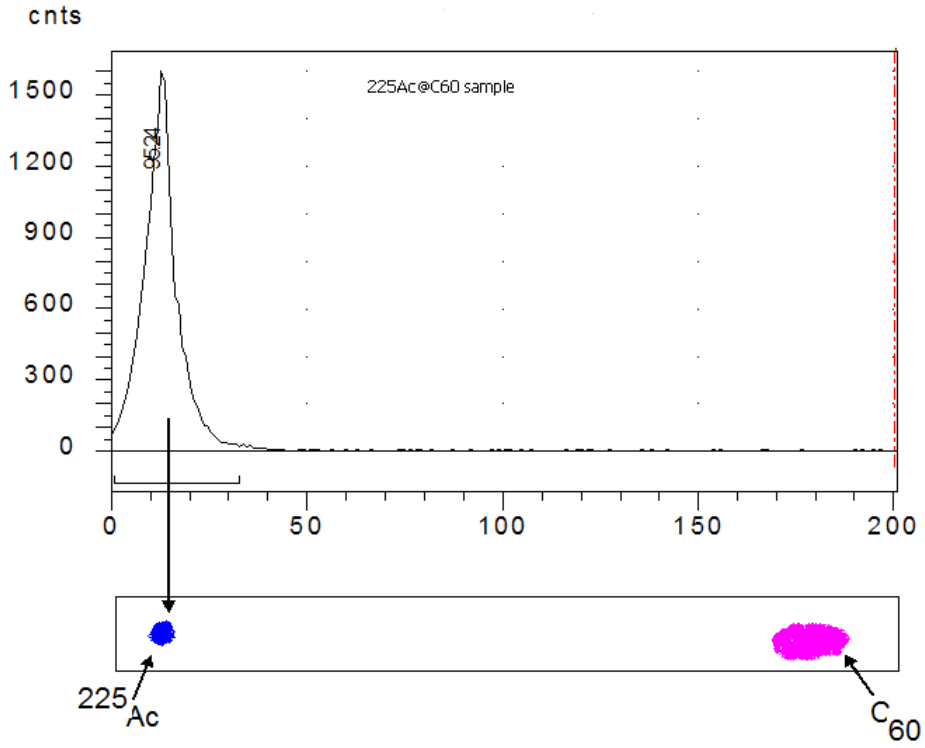

Figure 17: TLC radioanalyses of organic solution (Experiment 1)

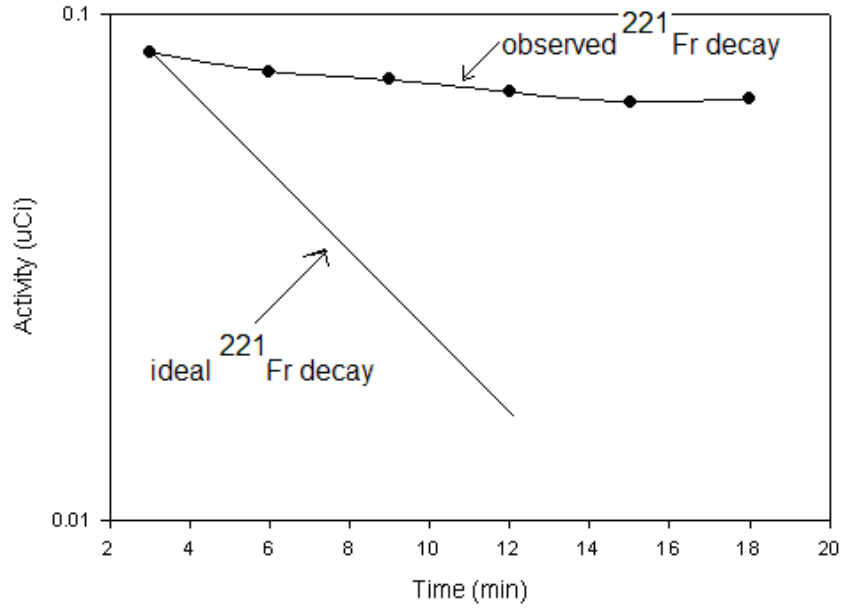

Figure 18: ^{221}Fr decay in aqueous solution

Table 7: Activity in aqueous extraction # 7

Date	**Time**	**Description of event**	**Assay of Radioactivity**							
			dT min	**shelf**	**Fr-221**			**Bi-213**		
					Counts	**uCi**	**%**	**counts**	**uCi**	**%**
11/19/06	3:19	Organic(before)	2	5	15.3	.240	100	25.8	.360	100
11/19/06	3:27	Extraction # 7 decay pattern ↓	2	5	5.36	.084	35	5.00	.069	19
11/19/06	3:29	↓	3	5	4.94	.077	32	5.02	.070	19
11/19/06	3:33	↓	3	5	4.67	.074	31	4.77	.066	18
11/19/06	3:36	↓	3	5	4.45	.070	29	5.16	.072	20
11/19/06	3:39	↓	3	5	4.26	.067	28	5.01	.070	19
11/19/06	3:42	↓	3	5	4.34	.068	28	4.91	.068	18
11/19/06	3:48	Organic (after)	3	5	10.9	.172	72	17.6	.246	68

Table 8: Activity in aqueous extraction # 8

DATE	TM	DESCRIPTION OF EVENT	**Assay of Radioactivity**							
			DT (min)	**Shelf**	**Fr-221**			**Bi-213**		
					Counts	**UCi**	**%**	**Counts**	**uCi**	**%**
11/19/06	1:1	Organic solution (before)	3	5	11	.173	100	11.3	.158	100
11/19/06	1:1	Extraction # 8 decay pattern ↓	2	5	4.0	.063	36	2.82	.039	24.6
11/19/06	1:2	↓	3	5	3.6	.056	32	2.75	.038	24.0
11/19/06	1:2	↓	3	5	3.8	.059	34	2.81	.039	24.6
11/19/06	1:2	↓	3	5	3.6	.056	32	2.92	.041	25.9
11/19/06	1:2	↓	3	5	3.5	.055	31	3.09	.043	27.2
11/19/06	1:3	↓	3	5	3.5	.055	31	4.30	.060	37.9
11/19/06	1:3	Organic (after)	3	5	7.0	.110	63	8.39	.117	74.0

Table 9: Activity in aqueous extraction # 9

DATE	TIME	DESCRIPTION OF EVENT	Assay of Radioactivity							
			DT (min)	**shelf**	**Fr-221**			**Bi-213**		
					counts	**uCi**	**%**	**counts**	**uCi**	**%**
11/19/06	1:38	Organic (before)	3	5	7.00	.110	100	8.39	.117	100
11/19/06	1:51	Extraction # 9 decay pattern ↓	2	5	1.85	.029	26	1.39	.019	16
11/19/06	1:53	↓	2	5	1.70	.027	24	1.26	.017	14
11/19/06	1:55	↓	2	5	1.66	.026	24	1.37	.019	16
11/19/06	1:58	↓	2	5	1.36	.021	19	1.39	.019	16
11/19/06	2:00	↓	2	5	1.37	.023	20	1.30	.018	15
11/19/06	2:02	↓	2	5	1.65	.026	24	1.41	.019	16
11/19/06	2:05	Organic (after)	2	5	6.31	.099	90	7.37	.103	88

Individual HPLC analyses of (1) a sample solution of C_{60} and (2) toluene solution suspected to contain $^{225}Ac@C_{60}$ provide spectra with the same retention time (Figure 19 and 20). When the eluted samples (2) from HPLC were radioanalysed, the ^{225}Ac activity was found not to correspond to the HPLC spectral peak at a 14 minutes retention time. When the malonate derivative of (2) was examined by HPLC, the result was peaks suggesting $^{225}Ac@C_{60}$ and $^{225}Ac@C_{60}$*malonate. The peak intensity corresponding to (2) decreased as the malonate peak was forming (Figure 21, 22, 23 and 24). The reaction was assumed to be completed as the starting materials peak ceased to exist (Figure 25).
Note: X stands for $^{225}Ac@C_{60}$,Y stands for $^{225}Ac@C_{60}$*malonate (unsaturated), and Z stands for $^{225}Ac@C_{60}$*malonate (saturated).

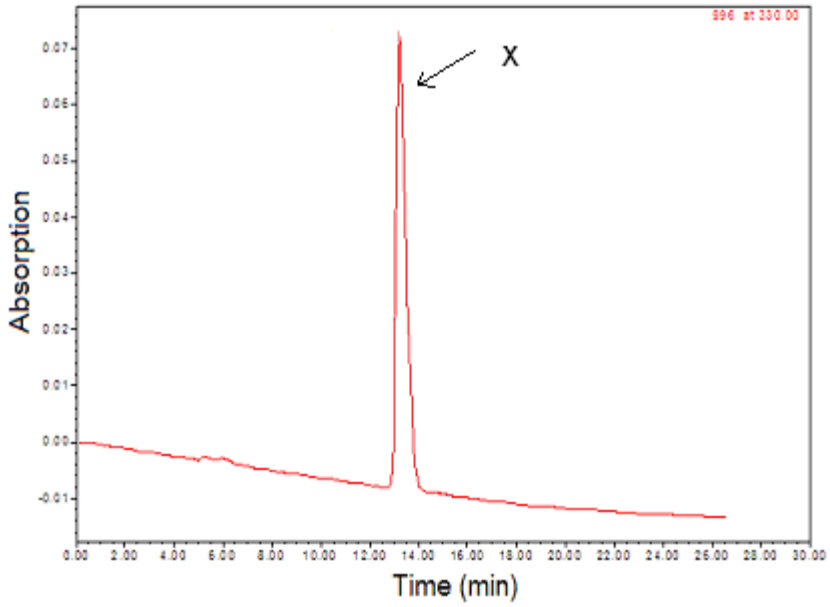

Figure 19: HPLC spectra of empty C_{60}

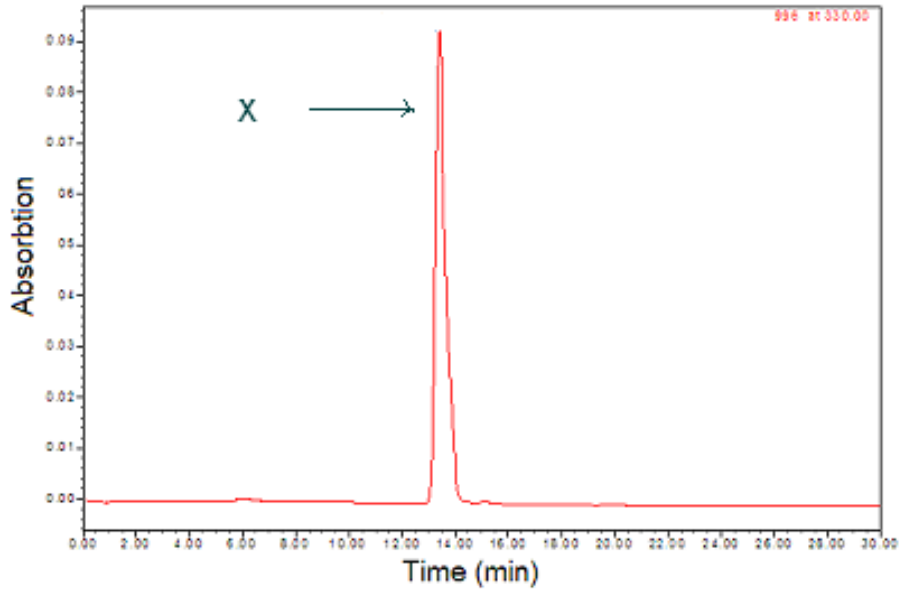

Figure 20: HPLC spectra of 225Ac@C_{60}

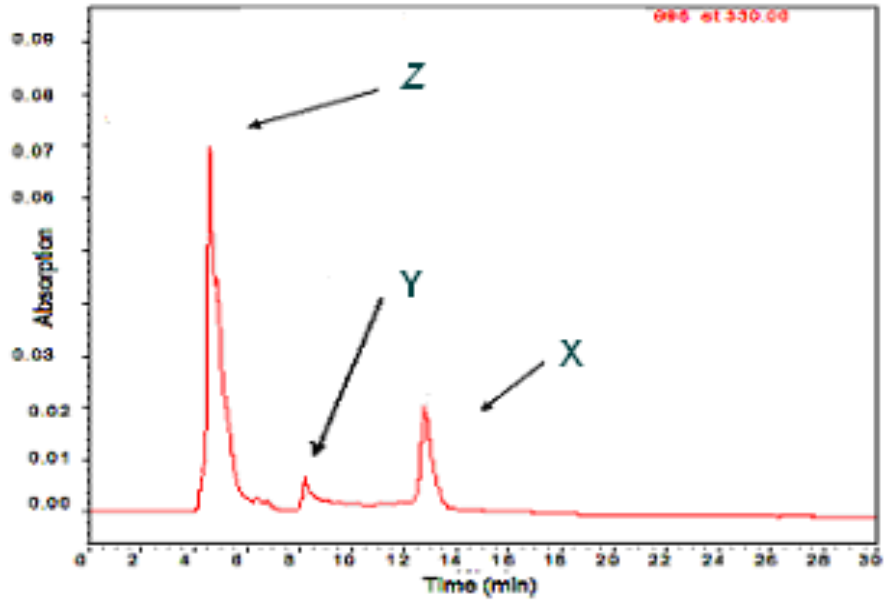

Figure 21: HPLC spectra of malonate formation (step 1)

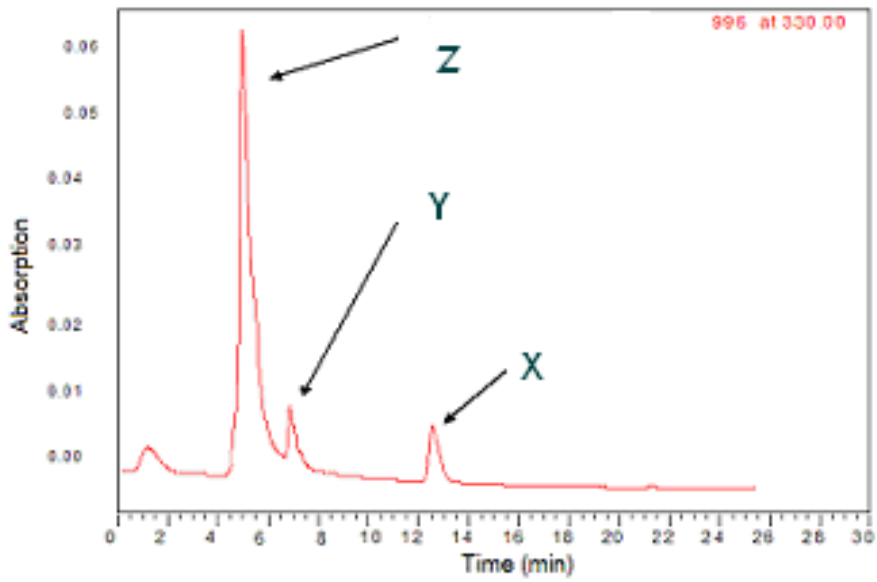

Figure 22: HPLC spectra of malonate formation (step 2)

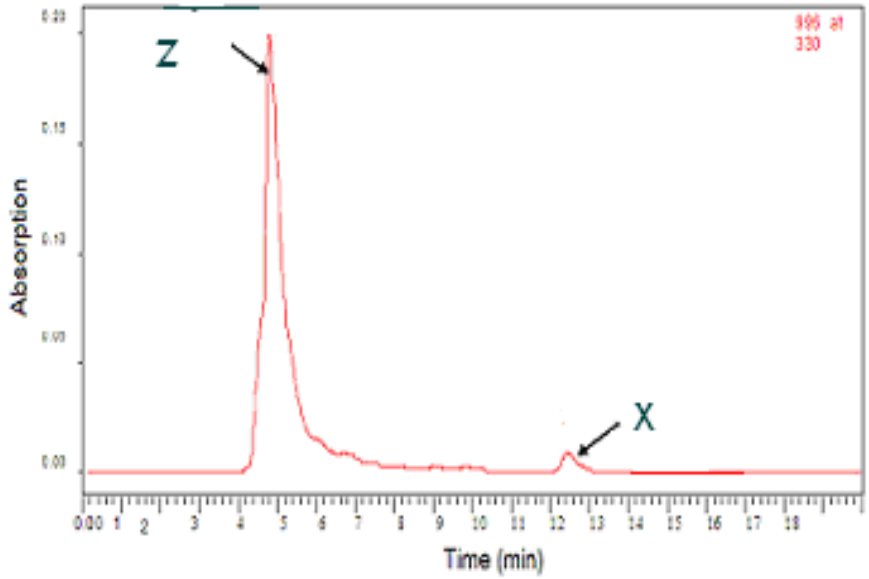

Figure 23: HPLC spectra of malonate formation (step 3)

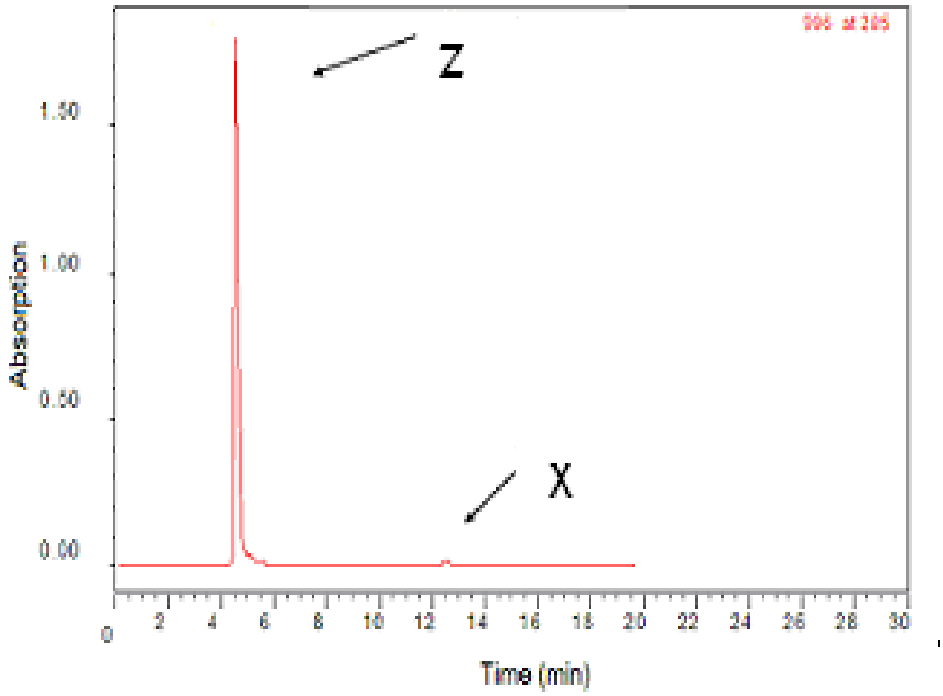

Figure 24: HPLC spectra of malonate formation (final step)

Successive liquid-liquid extractions (Figure 26) and radioanalyses of both phases (Figure 27 and Table 10) show that only 29% of ^{225}Ac (^{221}Fr) was initially extracted. Except to the first extraction, the ratio of the radioactivity of ^{225}Ac per extraction (Equation 1) was roughly 0.11 which suggests the existence of partition distribution constant K_d (Table 11 and Figure 28). Results demonstrate that subsequent to the first six extractions, 45 % of ^{225}Ac activity was still retained in the organic phase. The radioanalyses of aqueous phase extractions number seven, nine, eleven and thirteen (Figure 29 and Table 12, 13, 14 and 15), indicate that the decay pattern of ^{221}Fr activity (cps) follows its characteristic half-life. The analyses of the residual organic solutions using the TLC plate, (Figure 30) show evidence of radioactivity at 33 mm position as well as at the solvent front peak. Consecutive analyses of this plate 3 days afterward (Figure 30) revealed a decrease in the intensity of some of the previous peaks.

Equation 1 K_d = ^{225}Ac activity in aqueous phase/^{225}Ac activity in organic phase

Figure 25: Extractions from malonate

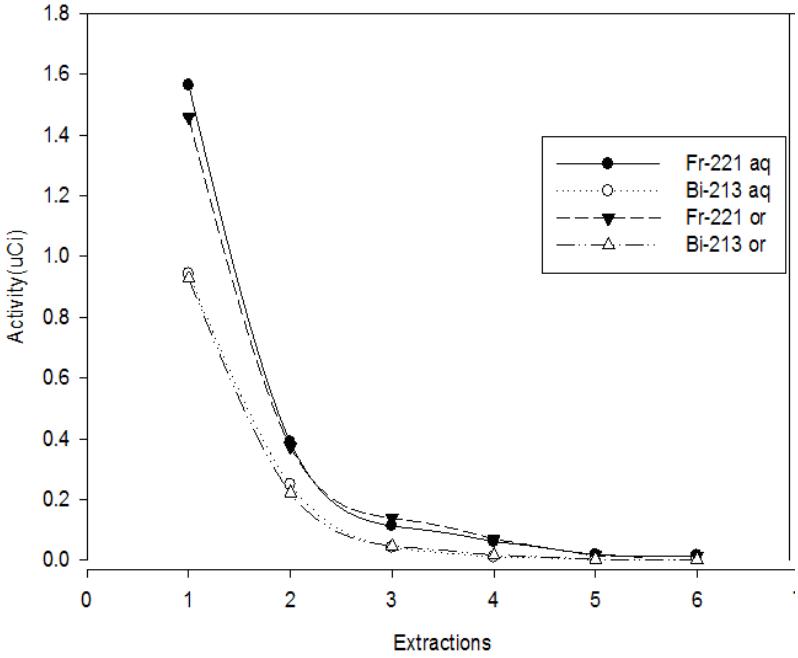

Figure 26: Activity distribution

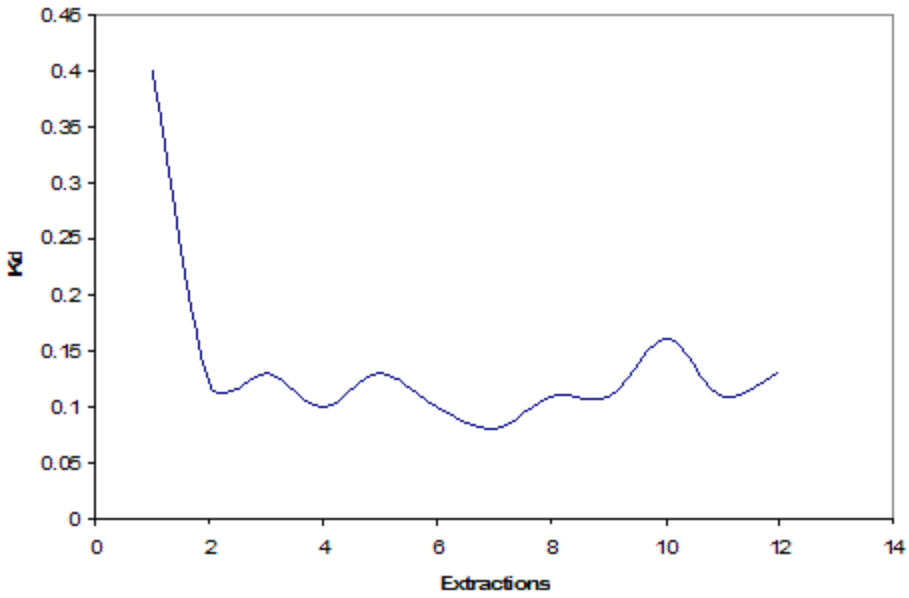

Figure 27: Partition coefficients Kd

Table 10: Fraction activity extracted from malonate solution

DATE	TIME	DESCRIPTION OF EVENT	ASSAY OF RADIOACTIVITY						
			dT (min)	Shelf	Fr 221				
					Total counts	% Error	Cps	uCi	% Extracted activity
12/23/06	12:35	Initial total Organic activity(5ml)	5	5	39200	0.67	1100	17.5	100
12/23/06	01:15	Aqueous # 1	2	5	37800	0.64	315	4.96	28
12/23/06	01:20	Aqueous#2	2	5	10400	1.23	86	1.36	7.9
12/23/06	01:24	Aqueous # 3	2	5	9740	1.20	82	1.27	7.4
12/23/06	01:29	Aqueous # 4	2	5	660	1.38	55	0.86	5.0
12/23/06	01:33	Aqueous # 5	2	5	7780	1.28	65	1.02	5.9
12/23/06	02:43	Aqueous # 6	2	5	6040	1.59	50	0.79	4.6
12/23/06	02:06	Aqueous # 7	2	5	5190	1.52	43	0.68	3.9
12/23/06	03:35	Aqueous # 8	2	5	3680	2.06	30	0.48	2.8
12/23/06	03:00	Aqueous#9	2	5	5290	1.60	44	0.69	3.9
12/23/06	04:16	Aqueous #10	2	5	4450	1.91	37	0.58	3.4
12/23/06	03:46	Aqueous #11	2	5	5600	1.48	47	0.73	4.2
12/23/06	04:50	Aqueous #12	3	5	5130	1.53	29	0.44	2.5
12/23/06	04:23	Aqueous #13	2	5	3360	2.56	28	0.40	2.5

Table 11 Distribution coefficient in malonate

time		Phase	Cps	Extracted			
Real T	min			% activity in organic solution	% activity in aqueous	Overall %	Kd=Aa/Ao
12:35	35	Organic 1	1100	100		100	.40
1:15	40	Aq# 1	315		28.6	29	
1:17	42	Organic 2	785	100		71.3	.11
1:20	45	Aq # 2	86.3		11	8	
1:21	46	Organic 3	698.7	100		63.5	.11
1:24	49	Aq#3	81.2		11.6	7.35	
1:26	51	Organic 4	617.5	100		56	.09
1:29	54	Aq #4	55		9	5	
1:30	55	Organic 5	562.5	100		51	.11
1:33	58	Aq # 5	64.9		11.5	5.9	
2:40	125	Organic 6	497.6	100		45	.10
2:43	128	Aq #6	50.3		10.1	4.57	
2:48	133	Organic 7	436	100		39.6	.08
2:06,2:38	112	Aq # 7	43.3,28.8		8.25	3.3	
2:55	140	Organic 8	399.95	100		36	.08
3:35	180	Aq#8	30.7		7.6	2.78	
3:29	174	Organic 9	388	100		35	.09
3/3:2	157	Aq 9	44.1,27.2		9.2	2.4	
4:05	210	Organic 10	329.2	100		29.9	.11
4:16	221	Aq 10	37.1		11.3	3.3	
4:11	216	Organic 11	280	100		25.4	.14
3:46,4:05	200	Aq 11	46.7,36.8		14.8	3.3	
4:45	249	Organic 12	245.4	100		22.3	.11
4:50	255	Aq 12	28.5		11.6	2.5	
4:46	251	Organic 13	212	100		19	.11
4:23,4:42		Aq 13	28,17		10.6	2	

Table 12: ^{221}Fr decay in aqueous extraction # 7

Time(real)	dT(analysis time)	Cps	uCi
2:06	2	43.2	.68
2:08	3	39.2	.62
2:11	3	34.8	.54
2:14	3	33.3	.52
2:18	3	31.1	.49
2:21	3	29.6	.46
2:24	3	29.5	.46
2:27	3	29.1	.45
2:31	3	28.6	.45
2:35	3	28.2	.44
2:38	3	28.8	.45
Analyzed Organic phase after extraction # 7			
2:48	3	436	6.87

Table 13: ^{221}Fr decay in aqueous extraction # 9

Time(real)	dT (analysis time)	Cps	uCi
3:00	2	44.1	.69
3:02	3	37.8	.59
3:05	3	34.4	.54
3:09	3	31.6	.49
3:12	3	29.6	.46
3:15	3	28.5	.44
3:18	3	27.8	.43
3:22	3	27.8	.43
3:25	3	27.2	.42
AQ extraction # 8 analyzed after # 9			
3:35	2	30.7	.48
Analyzed Organic phase after extraction # 9			
3:29	3	388	6.11

Table 14: ^{221}Fr decay in aqueous extraction # 11

Time(real)	dT(counting time)	Cps	uCi
3:46	2	46.7	.73
3:48	3	43.2	.68
3:52	3	39.8	.63
3:55	3	38.7	.61
3:58	3	37.8	.59
4:01	3	36.8	.58
4:05	3	36.8	.58
AQ extraction # 10 analyzed after # 11			
4:16	2	37.1	.58

Table 15: ^{221}Fr decay in aqueous extraction # 13

Time(real)	dT	Cps	uCi
4:23	2	28	.44
4:25	3	23.4	.36
4:29	3	20.8	.32
4:32	3	19	.29
4:35	3	18.3	.28
4:38	3	17.6	.27
4:42	3	17.0	.26
AQ extraction # 8 analyzed after # 12			
4:50	3	28.5	.44
Analyzed Organic phase after extraction # 13			
4:46	3	212	3.34

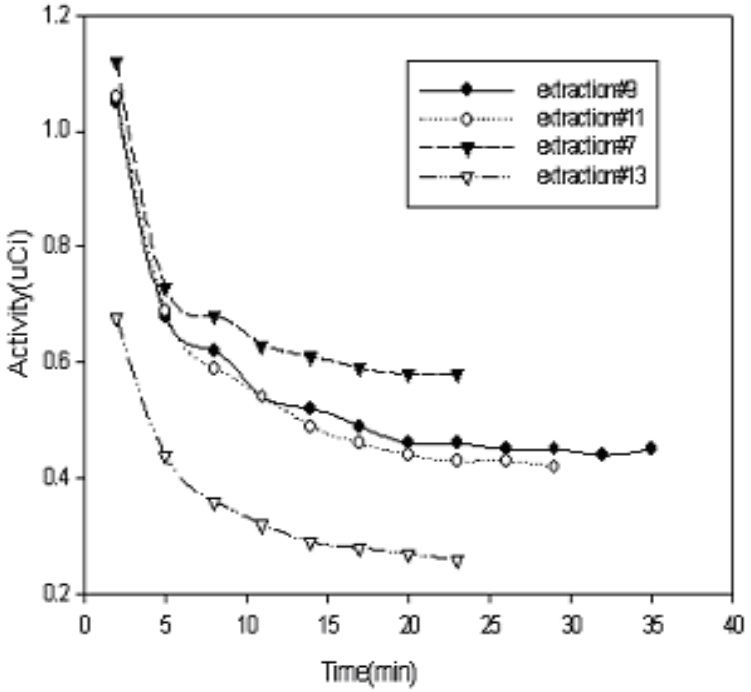

Figure 28: ^{221}Fr decay in aqueous extractions

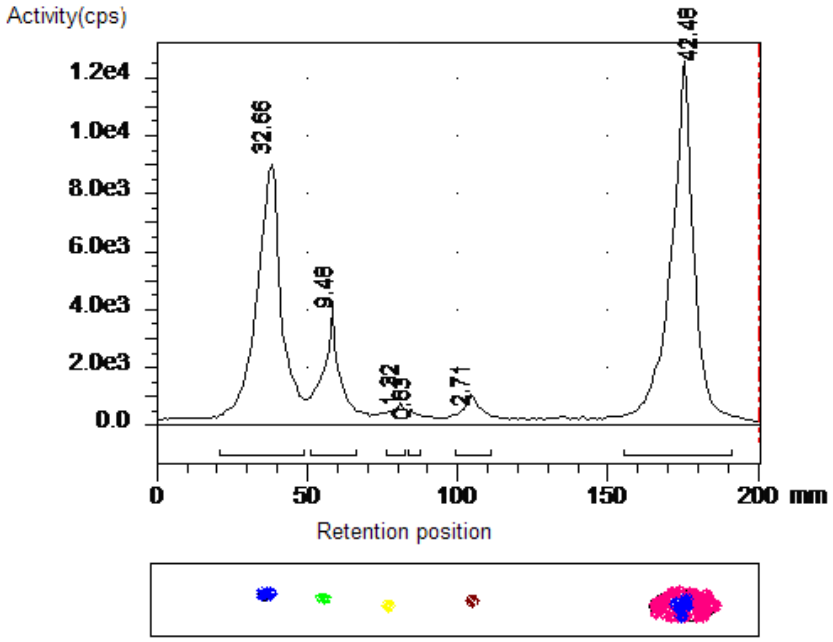

Figure 29: TLC spectra of malonate solution

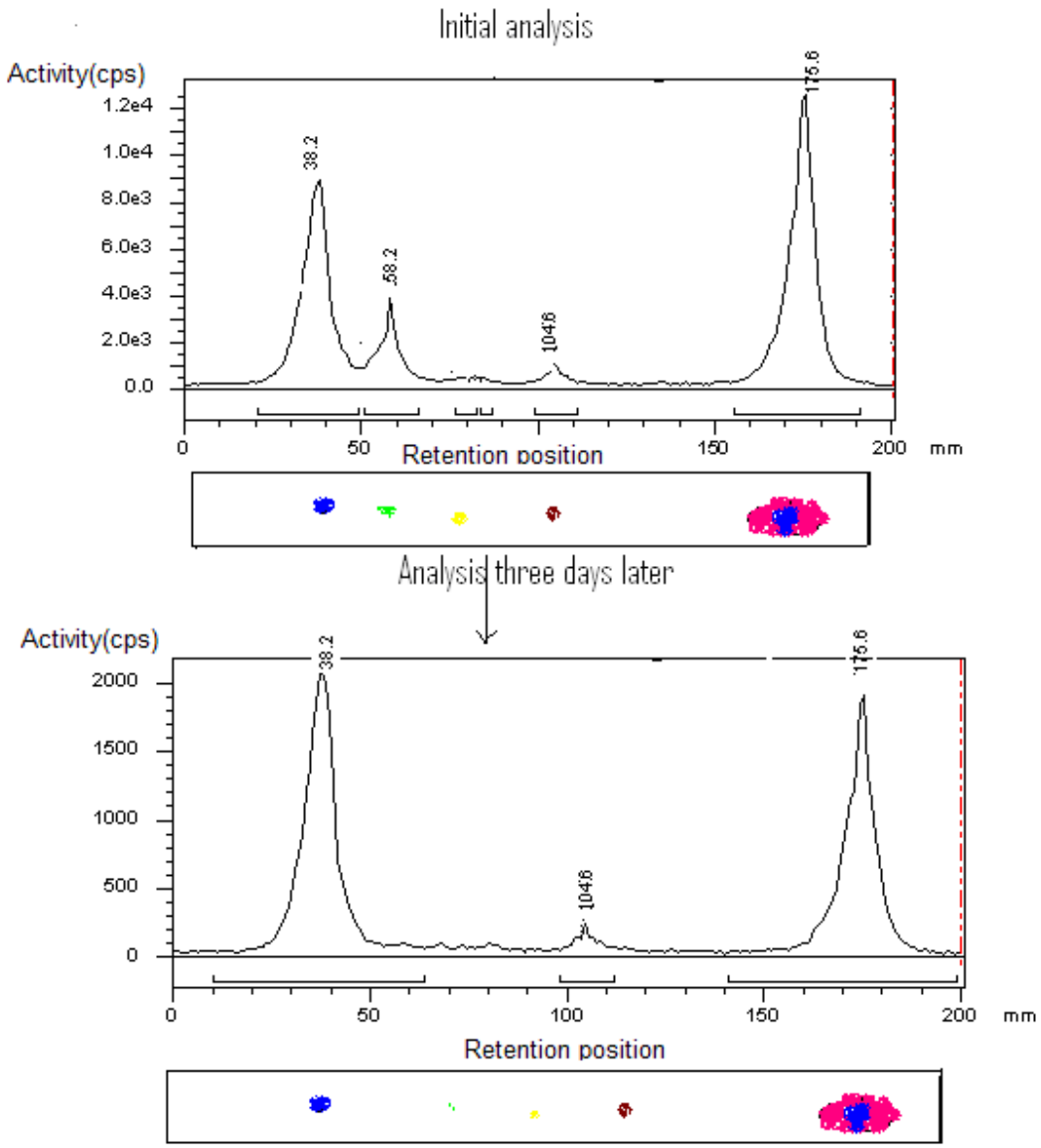

Figure 30: TLC spectra of malonate solution (3 days later)

CHAPTER 5

DISCUSSION AND CONCLUSION

5.1 Discussion

Endohedral metallofullerenes symbolized by $M@C_n$, is a class of novel materials that are made up of an atom or small compound or ion encapsulated within a fullerene cavity [12]. Fullerene molecules, represented by C_n (n = 20 – 120), are carbon-based nanostructures with a hollow spherical, ellipsoidal or cylindrical shape. Fullerenes are similar in structure to graphite, which is composed of a sheet of linked hexagonal rings, but they also contain pentagonal (or sometimes heptagonal) rings that prevent the sheet from being planar [5]. Numerous techniques for the insertion of a foreign atom or ion into fullerene have been reported. While most Group 2 and 3 elements can be incorporated into fullerenes during the gas-phase synthesis of the fullerene, encapsulation of most of the other elements requires forcing the element through the fullerene cage by one means or another [14]. Most of the known chemistry of endohedral metallofullerenes has concerned lanthanide and alkaline earth metals, with a few reports of actinide encapsulation [15]. The first large scale preparation of metalofullurenes ($La@C_{60}$) was demonstrated by Chai, et al. using a D.C. arc discharge method of doped graphite [16]. Theoretical calculations of $La@C_{60}$ by Nagase, et al. strongly suggest that there is a charge transfer between the central atom and the fullerene cage, i.e., its electronic structure could be described as $La^{3+}C^{3-}{}_{60}$ [17]. Further measurements of the nuclear-spin properties of La atom within this molecule by Suzuki, et al. and Johnson, et al. strongly suggest that the metal was trapped inside fullerene cage [18, 19]. However, because of the periodic-table relationship between La and Ac it is possible that ^{225}Ac inside C_{60} will behave similarly to La inside C_{60}. In addition, a report by Wan, et al. demonstrated the synthesis of $[Na@C_{60}]^+$ by collision of alkali-metal ions with C_{60} [20]. Under high pressure and high temperature conditions, Saunders, et al. incorporated noble gas atoms into fullerene [21]. Braun, et al. use the recoil of gamma-ray emission to synthesize metal

atom containing endohedral fullerenes [22]. However, it has been pointed out by Kikuchi, et al. that it is not clear whether the endohedral form is stable as an isolated free molecule [13]. In response to this argument, studies by Smalley's group illustrate that this species would fragment through sequential loss of C_2 until the cavity space of fullerene is not sufficient enough to encapsulate the metal atom or ion [5, 16]. In other words, the tendency of multiple C_2 elimination from the fullerene would terminate when the fullerene molecular size approaches the size of an encapsulated metal atom. One of the intriguing uses of fullerenes in nuclear medicine would be encapsulation of radioisotopes which are unsuited to traditional methods for in vivo transport. Significant progress has been made towards intercalating stable atoms into the fullerene lattice. This is achieved by neutron activation of the gas atoms, and allows it to recoil followed by prompt gamma-ray emission to incorporate the product nuclide into the fullerene [24]. However, the isotopes created in these experiments so far do not have obvious uses in nuclear medicine. Also, there are no simple neutron activation pathways that lead to alpha-emitting radioisotopes of interest. Other techniques for the encapsulation of atoms into fullerene include laser ablation methods and chemical synthesis methods. Drawbacks of these methods include: complex instrumentation, high current (100-200 A), dissipated heat, and the need of cooling mechanisms [14]. For these reasons and that mentioned earlier, a new approach has been taken. This new approach was used to investigate the molecular stability of synthesized $^{225}Ac@C_{60}$ and the fate of its decay products. For in vivo applications, the study of the molecular stability of $^{225}Ac@C_{60}$ is critical in determining whether the fullerene ligand could prevent direct binding of the ^{225}Ac (toxic radionuclide) with serum components and tissue by providing a thermodynamically stable molecular environment. The fate of decay products provides information on possible pathways in which encapsulated radionuclides might escape from the fullerene cage. This approach is different from conventional methods because it uses fullerene as a starting material. It also takes advantage of advancements in the fullerene industry for its achievement in massive production of C_{60} [23]. In addition, it considers that the amount of ^{225}Ac that was available for single experiment trial was in the range of 1.5 mCi to 2 mCi ≈ (< $10^{\wedge -10}$ g), which was too little to be used in convectional methods for

synthesizing M@C_{60}. Part of the appeal of this method is that it can be performed on very small scale, without vacuum apparatus, and without aerosolizing radioisotopes as would occur by standard electric arc or the laser ablation process for generating endohedral metallofullerenes. Electroplating of ^{225}Ac on Pt electrode was a step towards the synthesis of ^{225}Ac@C_{60}. In general, over 70% of ^{225}Ac was electroplated (^{225}Ac target), which was found to be enough to carry out the electric arc experiment. The target was then subjected to a high potential-direct current electrical arc chamber for the insertion of ^{225}Ac into the fullerene cavity to form ^{225}Ac@C_{60}. Results from liquid-liquid extractions followed by chromatography analyses of the toluene solution that was suspected to contain endohedral ^{225}Ac@C_{60} demonstrated that some of ^{225}Ac could not be extracted from the organic phase. It is our presumption that this radioactivity in the toluene solvent was due to the endohedral ^{225}Ac@C_{60}. We have shown in Chapter 1 that the recoil energy of alpha particle from ^{225}Ac is 0.1 MeV. This energy is extremely high compared to the bond energies associated with C-C atoms in C_{60} (3 keV). We propose that the high recoil energy of alpha particle allows the trapped daughter nuclear to recoil out of the fullerene cage (Figure 31). This notion is supported by the TLC results that the ^{225}Ac radioactivity remained unmoved. However, still some serious arguments remain whether the residence time of ^{225}Ac in C_{60} is shorter than the time in which ^{225}Ac@C_{60} dissociates into individual components. If this is true, it implies that the time between extractions, and the time required to develop the chromatography plate is enough for the ^{225}Ac@C_{60} to decompose into individual components. In other words, by the time extractions and chromatography were completed, ^{225}Ac exists as an unsealed radioactive source. The tendency of ^{221}Fr activity (cps) to remained almost unchanged (extractions seven – nine) confirms that ^{225}Ac has escaped from the cage. We propose that the path in which entrapped ^{225}Ac released from the cage is through the chemical dissociation of fullerene as proposed by Smalley, et al. It has been reported by Hirsch, et al. that fullerene can be chemically modified by a large variety of addition reactions, which allow the combinations of its properties with those of other class of materials [14]. Nucleophilic cycloaddition reaction (Bingel) of C_{60} was selected as synthetic methodology to organize ^{225}Ac@C_{60} into three dimensional networks [27]. The toluene solution that was suspected

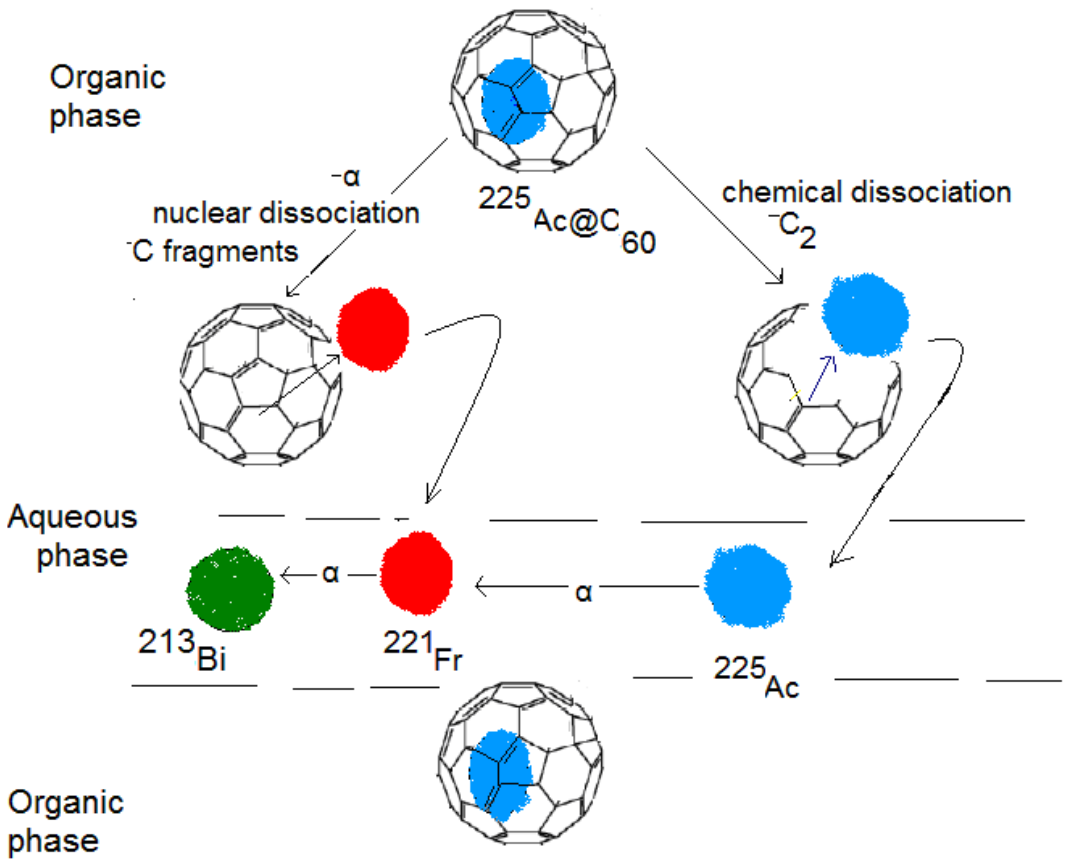

Figure 31: Escape mechanisms

to contain $^{225}Ac@C_{60}$ and empty fullerene were used as starting materials. This transformation was accompanied by a vigorous gas evolution and quantitative precipitation of sodium salt. Results demonstrate that subsequent to the first six extractions, 45 % of ^{225}Ac activity was still retained in the organic phase. The increase in encapsulation efficiency resulted from the improvement in structural stability by converting SP^2 hybrid carbon to SP^3. In addition, further evidence for endohedral formation was found in the analyses of the residual organic solutions using the TLC plate, which showed evidence of radioactivity at the same position where fullerene malonate was located. Based on the peak intensity depreciation rate (TLC spectra) as the function of time, the successive analyses of the same plate would suggest the possible half lives of the nuclides present in that particular plate. To pin point that a particular peak corresponded to ^{213}Bi (t ½ = 45.6 min), the TLC plate was subjected to analyses at 3 hour time intervals. The peaks that were observed to decay with a characteristic half- life of 45.6 min, confirmed the presence of ^{213}Bi. However, in this time window, the peaks intensity that were observed to remain unchanged, suggested the presence of ^{225}Ac (t ½ = 10 d). In order to identify the peaks that corresponded to ^{221}Fr (t ½ = 4.8 min), TLC plates were subjected to short time analyses of 2 min intervals for a period of 20 min. The consecutive analyses of this plate 3 days later revealed peaks with intensity decrease with 10 days half life, which confirm the presence of ^{225}Ac. The process of nuclear dissociation event (^{225}Ac decay to ^{221}Fr), was observed independently from the fullerene chemical dissociation in short-time analyses of the aqueous solution resulted from two-fast (back to back) extractions from residual solution. The 1st extraction (among the two-fast extractions) serves the purpose of removing most of ^{225}Ac resulting from fullerene chemical dissociation. The short time analyses of ^{221}Fr activity in the 2nd extraction revealed the decay pattern of ^{221}Fr (half life 4.8 minutes). When the decay curve was sorted-out into individual components, it was found that radioactivity due to ^{225}Ac added to the total background [Figure 32]. At any point on the curve, the total radioactivity is the summation of ^{221}Fr activity and ^{225}Ac activity. Additional evidence of endohedral ^{225}Ac metallofullerenes was supported by the results from the reverse-electrolysis experiments of ^{225}Ac-fullerene catcher disk-electrode. The fullerene catcher disk

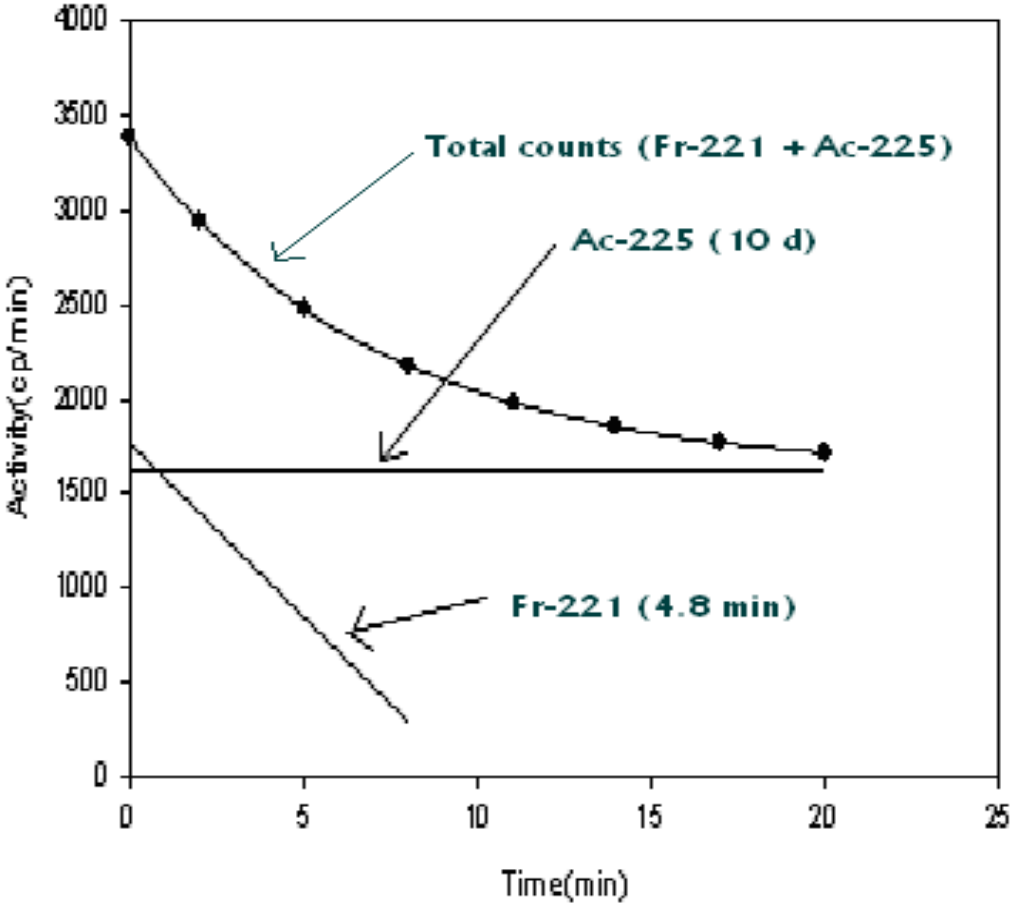

Figure 32: ^{225}Ac background

electrode, which was suspected to contain $^{225}Ac@C_{60}$ (in the course of arcing event), was placed in electrolysis set-up. This electrode was connected to the (+Ve) terminal of a power supply, and mesh-like Pt electrode (Chapter 2) was used as counter electrode in dilute acid solution. The main idea was to investigate the form in which ^{225}Ac exist in ^{225}Ac-fullerene catcher disk-electrode, i.e. whether it was ionic or non-ionic form? Stipulation that ^{225}Ac deposit in ^{225}Ac-fullerene catcher disk-electrode was ionic, it would migrate to the (-Ve) electrode. However, if ^{225}Ac deposits on ^{225}Ac-fullerene catcher disk-electrode failed to migrate to counter electrode, it would suggest that ^{225}Ac in ^{225}Ac-fullerene catcher disk-electrode was not ionic, probably it exist as $^{225}Ac@C_{60}$. The results indicated that after two hours of the reverse electrolysis, significant amounts of the ^{225}Ac radioactivity was left on fullerene-catcher-disk electrode, suggesting that the ^{225}Ac was not ionic, hence $^{225}Ac@C_{60}$. The arcing-insertion methodology for put in ^{225}Ac in C_{60} (Chapter 3) was validated using stable isotope of Gd. The organic solution that suspected to contain $Gd@C_{60}$ was digested with H_2O_2 then submitted for Inductive Coupled Plasma (ICP) mass analyses. The results indicated that Gd was present, which prove that the technique was working.

5.2 Conclusion

Experiments were carried out to ascertain if ^{225}Ac would attach to the 3-dimensional C of fullerene. No attachment was detected, providing confidence that ^{225}Ac would not attach to the exterior of the C_{60} cage. Attempts were made to incorporate ^{225}Ac in C_{60} by performing an electric arc discharged between an Al disk with a C_{60} coating and a Pt disc onto which ^{225}Ac had been electroplated. The materials on the Al disk were dissolved in toluene. This organic phase was subjected to a series of washings with dilute HNO_3. These washings were analyzed to for ^{225}Ac, ^{221}Fr and ^{213}Bi. It was discovered that 99% of the activity of the original organic phase had been removed. The sources of ^{225}Ac in the aqueous phases could be: (a) ^{225}Ac was not incorporated in the C_{60} , (b) ^{225}Ac was incorporated in the C_{60}, then escaped by disrupting the cage. The sources of the ^{221}Fr

could be: (1) ^{221}Fr came from the decay of ^{225}Ac which had not been incorporated in the C_{60}, (2) ^{221}Fr came from the ^{225}Ac incorporated in the cage and then escaped from the cage, (3) ^{221}Fr came from ^{225}Ac incorporated in the cage and the decay recoil drove it through the cage. The above toluene phase was washed with dilute HNO_3 to remove all species that were water extractable, leaving only $^{225}Ac@C_{60}$. To this organic phase, a period of 30 min interval was allowed to lapse between 3 extractions. These 3 washings were analyzed for ^{221}Fr in short time analyses of 2 min for periods of 20 to 30 min. The ^{221}Fr decay curves all showed a very-slight down slope indicating that the ^{221}Fr was in equilibrium with ^{225}Ac. This parent – daughter equilibrium phenomenon could be brought about by the resultant effect of some of the above mechanisms. A portion of organic solution that contained $^{225}Ac@C_{60}$ was subjected to TLC and HPLC. The TLC analyses showed that the activities and C_{60} did not migrate together, indicating that the ^{225}Ac had been released from the cage, suggesting that $^{225}Ac@C_{60}$ is an unstable structure. The HPLC analyses yielded no further information. Attempts were made to improve the structural stability of $^{225}Ac@C_{60}$ and to investigate the fate of $^{225}Ac/^{221}Fr$ escape mechanisms. This was accomplished by taking endohedral $^{225}Ac@C_{60}$ from the Al catcher disk and dissolving it in toluene, then converting it to the malonic ester derivative under N_2. The organic solution was then subjected to the same treatment as described earlier. After the first 6 washes, 45% of the original activity remained in the organic phase, indicating that the surface alteration on $^{225}Ac@C_{60}$ had enhanced the structural stability significantly. This organic solution was further subjected to 8 uninterrupted succeeding extractions consisting of four pairs of two back to back extractions. For every single extraction, the first wash was discarded and the second wash was analyzed for ^{221}Fr over a period of 20 min. The ^{221}Fr activities in the samples decayed with the characteristic half life of the nuclide ($t_{½}$ = 4.8 m). This indicated that the third mechanism (3) was operating. The portion of organic solution that contained $^{225}Ac@C_{60}$*malonate was subjected to both TLC and HPLC analyses. TLC analyses showed a peak that indicated the presence of $^{225}Ac@C_{60}$*malonate. The HPLC analyses showed a separation between $^{225}Ac@C_{60}$*malonate from $^{225}Ac@C_{60}$.

REFERENCE

1. Juweid, M. E. *J Nucl Med*, **2002,** *43*, 1507-29.

2. Cagle, D; Kennel, S; Mirzadeh, S; Alford, J; Wilson, L. *Proc.Natl.Acad.Sci*. **1999,** *96*, 5182.

3. Henriksen, G. Radiochimica Acta. 2003, 91, 109-14.

4.Smith, S; Bartolo, N; Mirzadeh, S; Lambrecht, R; Knapp, F: Hetherington, E. *Appl. Radiat. Isot.* **1995**, *46*, 8.

5. Kroto, H.W; Heath, J.R; O'Brien, S.C; Curl, R.F; Smalley, R.E. *Nature* **1985,** *318*, 162- 163.

6. Bezmel'nitsyn, V.N; Eletskiĭ, A.V; Okun', M.V. *Uspekhi Fizicheskikh Nauk*, Russian Academy of Sciences, **1998**, *41*.

7 Wudl, F. *J. Mater. Chem*, **2002**, *12*, 1959–1963

8. Taylor, R. *J. Chem. Soc* . **2002**, *2*, 41 – 46.

9. Kennel, S. **Cancer Research.** *1991*, 51, *1529-1536.*

10. Salame, M.Y. *European Heart Journal.* **2001** *22(8)*, 629-647

11. a. Taylor, R; Walton, D.R.M. *Nature*, **1993**, *363*, 685; b. Hirsch, A. *Angew. Chem. Int. Ed. Engl*., **1993**, *32*, 1138; c. Schwarz, H. *Angew. Chem. Int. Ed. Engl.*, **1992**, *31*, 292.

12. Wudl, F; Hirsch, A; Khemani, K.C; Suzuki, T; Allemand, P.M; Koch, A; Eckert, H; Srdanov, G; Webb, H.M; in *Fullerenes: Synthesis, Properties, and Chemistry of Large Carbon Clusters;* Hammond, G.S and Kuck, V.J Eds., ACS: Washington, DC, **1992**, *481*, 161.

13 Kikuchi, K; Ohtsuki,T; Nagame, Y; Katada, M; Nakahara,H.*J. Radioanal. Nucl. Chem*.**2002** 31.

14. Diener, M. D; Alford, J. M; Kennel, S. J; Mirzadeh, S. *J Am Chem Soc*. **2007,** *25*, 129 (16), 5131-8.

15. Gu, T; Diener, M. D; Chai, T; Smalley, R.E. *Science* **1992** , *257* ,1661-3.

16. Chai, Y; Guo, T; Jin, C; Haufler, R.E; Chibante, L.P.F; Fure, J; Wang, L; Alford, J.M; Smalley, R.E. *J. Phys. Chem.* **1991**, *95*, 7564

17. Nagase, S. *Bull. Chem. Soc. Jpn.* **1996,** *69*, 2131-2142.

18. Johnson, R.D; de Vries, M.S; Yannoni, S. *Nature.* **1992,** *355*, 239.

19. Suzuki, S; Kawata, S; Shiromura, H; Yamauchi, K; Kikuchi, K; Kato, T Achiba, Y. *J.Phys.Chem.* **1992**, *96*, 7159.

20. Wan, Z; *Phys.Rev.Lett*. **1992**, 69, 1352.

21 Syamala, M; Cross,R; Saunders,m. *J.Am.Chem.Soc*, **2002** ,124,6216.

22 Braun,T; Rausch.H. *Chem.Phys.Letters* 1995, 237, 443-447.

23 Kasumov, M.; Pokropivny, V. *Tech.Phy*. **2007,** 52 , 956-958(3).

24 Braun. T; Rausch. H. Chem. Phy. Letters. 1999, 179 – 182.

VITA

Jofa Gideon Mwakisege was born in Morogoro, Tanzania. Jofa joined Tambaza High School in 1997 where he graduated with honors on June 1999. Upon graduating he joined the Butler County College where he stayed for two years then transferred to Newman University, where he graduated with BS in Chemistry in May 2004. In 2004, Jofa started his graduate studies at University of Tennessee in Chemistry working on catalysis under Dr. Zhang. In 2005, he joined Nuclear Medicine group – Oak Ridge National Laboratory working on radiochemistry under the supervision of Dr. Saed Mirzadeh. In the final year of his graduate studies, Jofa explored the utilization of organometallic chemistry to chelate radionuclides. Upon his graduation from U.T.K, Jofa plan to pursue the PhD in Nuclear Engineering.